11-18-1992

Dynamic NMR Study of Bond Rotational Activation Parameters in Micelles

Dietmar A. Leitner
Portland State University

AN ABSTRACT OF THE THESIS OF Dietmar A. Leitner for the Master of Science in Chemistry presented November 18, 1992.

Title: Dynamic NMR Study of Bond Rotational Activation Parameters in Micelles.

APPROVED BY THE MEMBERS OF THE COMMITTEE:

[redacted]
David H. Peyton, Chair

[redacted]
Gordon Kilgour

[redacted]
Alfred Levinson

[redacted]
Robert L. Millette

The behavior of surfactants in solution has been and still is of scientific, technological, and industrial interest. The micelle forming compounds sodium N-(octyloxycarbonyl)sarcosinate (NaOcSarc), and sodium N-(decyloxycarbonyl)sarcosinate (NaDecSarc) show in aqueous solution two ^{1}H NMR N-methyl peaks arising from a possible cis- or trans-conformation. The relative population of the N-methyl peaks depends mostly on the concentration of surfactant indicating micelle formation. Upon heating the two peaks start to coalesce and finally appear as one single peak . The temperature range in which this phenomenon occurs is from 25°C to 65°C. The primary interest of this study

was to determine the activation parameters of rotation about the carbonyl-nitrogen (C-N) bond. Dynamic nuclear magnetic resonance spectroscopy was employed to approach this problem. A complete bandshape analysis was performed in order to calculate the free energy ($\Delta G^{\ddagger}$), enthalpy ($\Delta H^{\ddagger}$), and entropy ($\Delta S^{\ddagger}$) of activation. The effect of a different counter ion (Li^{+}) and sodium chloride salt addition were tested for possible changes of the activation parameters. Studies in nonaqeous solvents were conducted with the free acid form of the mentioned carbamates. Dimethylsulfoxide and chloroform were chosen as organic solvents for these particular experiments. The critical micellar concentrations of all surfactants were determined, and the assignment of the individual N-methyl peaks to the correspondend conformation could be unambiguously shown by a two dimensional NMR experiment.

The cmc's show strong salt dependence. The effect of a lithium as an alternative counter ion has a less drastic effect. Micellization seems not to occur in the free acid cases.

Interestingly, the surfactants show stronger salt dependence than micellization dependence upon the activation parameters, indicating that solvent exposure occurs at the C-N partial double bond and considerable deformation of the ideal spherical shape.

DYNAMIC NMR STUDY OF BOND ROTATIONAL ACTIVATION PARAMETERS IN MICELLES

by

DIETMAR A. LEITNER

A thesis submitted in partial fulfillment of the
requirements for the degree of

MASTER OF SCIENCE
in
CHEMISTRY

Portland State University
1993

TO THE OFFICE OF GRADUATE STUDIES:

The member of the Committee approve the thesis of Dietmar Leitner presented November 18, 1992.

[redacted]
David H. Peyton, Chair

[redacted]
Gordon Kilgour

[redacted]
Alfred Levinson

[redacted]
Robert L. Millette

APPROVED:

[redacted]
Gary Gard, Chair, Department of Chemistry

[redacted]
Roy W. Koch, Vice Provost for Graduate Studies and Research

ACKNOWLEDGMENTS

The preparation of this document was certainly positively influenced by many people and factors. Trying to mention everybody would be a total failure in the sense of completeness.

However I like to thank my advisor Dr. Peyton for his time, suggestions, and support, especially in the final stretch of this effort. Furthermore I want to acknowledge the patience my parents had with their son who extended his stay in the US innumerous times and their never ending willingness to support me.

TABLE OF CONTENTS

LIST OF TABLES

LIST OF FIGURES

CHAPTER I

INTRODUCTION

The behavior of surfactants in solution is still a subject of scientific, technological, and industrial interest (1 - 5). After decades of research, many questions such as micelle formation, structure, and dynamics are only partly answered and remain topics of scientific discourse. At this point it seems to be generally accepted that these structures include a hydrophobic core region from which water is largely absent; outside this nucleus some fraction of the remaining hydrocarbon and the polar head group of each detergent molecule are in contact with water to some degree. A fluidity gradient is observed as one progresses from the head-group region to the tail, with motion becoming freer as the tail is approached. These conclusions are similar to observations made with lipid bilayers and biological membranes. In these systems the polar surface is highly ordered, and molecular motion increases in rate and amplitude as the more hydrophobic interior of the structure is approached (6).

This thesis focuses on the kinetics of the inter conversion between conformational isomers in micelles, as a model for biological membranes. There is evidence that the relative conformational energies of the two forms of the amide functional group (Figure 1a, 1b) are altered when this group is present at the surface of a micelle, increasing the population of the trans isomer (Figure 1a) relative to the cis form (Figure 1b) substantially.

Previous work (7) has shown that the kinetics of rotation of an amide group in sodium N-octanoyl sarcosinate (SNOS) is too slow to be studied by NMR lineshape analysis in water as a solvent. Therefore carbamates (Figure 2a, 2b) were chosen, because they have a reduced activation barrier of rotation about the carbonyl-nitrogen (C-N) bond (8) due to the

extra oxygen. The micelle forming compound sodium N-(octyloxycarbonyl)sarcosinate (NaOcSarc) and other related carbamates were synthesized and their activation parameters of rotation about the carbonyl carbon-nitrogen bond were measured by proton nuclear magnetic resonance techniques (^{1}H NMR).

The rate of exchange (k) between conformations of these carbamates were determined by the complete band shape (CBS) method (9, 10). The activation parameters can be calculated from the slope and intercepts of a resulting plot of log(k/temperature) vs 1/temperature (11). The rotation about the C-N bond in the carbamates leads to a set of very temperature-sensitive spectra in the region 293 K- 338 K. This allows reliable line fits, as opposed to the analogous amides, which show hardly any temperature-dependence in this range.

The obtained spectra indicate a predominant cis conformer in the nonmicellar state, and a predominant trans conformer in micellar state. The effect of varying the chain length, a different cation (Li^+) and the presence of salt (NaCl) on the cmc and the activation parameters was studied. Also, the protonated free acid was investigated in dimethylsulfoxide (DMSO) and chloroform as solvents.

This study should give insight and better understanding of the parameters influencing the internal motions of a molecule, including their magnitudes. The C-N bond in carbamates proves to be a sensitive probe for this purpose. Results might apply qualitatively to biological membranes because micelles are considered to be model systems for biological systems.

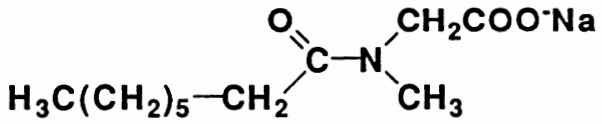

1a (trans-conformation)

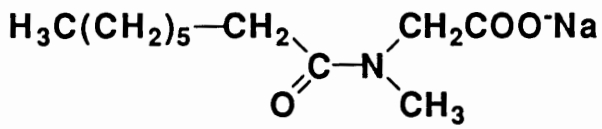

1b (cis-conformation)

Figure 1. Two possible conformational structures of SNOS (1a, 1b).

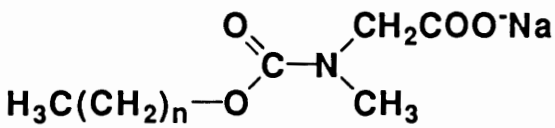

2a (trans-conformation)

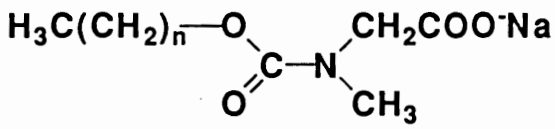

2b (cis-conformation)

Figure 2. Two possible conformational structures of the corresponding carbamates (2a, 2b) to (1a, 1b).

CHAPTER II

REVIEW OF THE LITERATURE

HISTORY AND TERMINOLOGY

The behavior of amphiphiles in water and other polar or even nonpolar solvents has a long and honorable history. The word amphiphile (from Greek, "amphi" means of both kinds and "philos" means strong affinity, attraction, or love) describes the presence of both hydrophilic and hydrophobic parts within the same molecule. The resulting unique properties, which do not follow the patterns of solution behavior common to most solutes as their concentration is increased, raised scientific interest even before this century.

A report from Benjamin Franklin exists (12), describing him pouring a teaspoonful of "oil" on the rough surface of a large pond around the year 1770. He was surprised that the smoothening effect due to the surface active properties of the oil of such a small volume spread out over a large area that he estimated as 2000 m^2. Although he did not realize that he actually measured one molecular parameter, he understood that the spread of the smoothening effect was of higher scientific importance than the effect itself. In his report he tried to comprehend the observed phenomena but he could not explain it to his full satisfaction.

In 1890 Lord Rayleigh (13) quantified Franklin's experiment in his laboratory and draw the conclusion that the film thickness must be around 1.7 nm. This was the first estimate of this molecular parameter to such high precision.

J. W. Mc Bain (14) suggested in 1914 that individual molecules in solution can aggregate into clusters, named micelles (from the Latin word, micella, meaning small bit),

above a characteristic concentration. The characteristic concentration is called the critical micelle concentration (abbreviated cmc). Since then a vast number of papers dealing with empirical and theoretical aspects of the behavior of micelles in solution has been published.

Trying to explain the association mechanism of micelles, and presenting the first geometrical model of micelles as spheres, G. S. Hartley (15) is acknowledged as one of the pioneers in this field. Hartley published his famous book on micelles in 1936.

By using elastic light scattering, P. Debye (16) introduced a still-useful method to determine aggregation numbers of micelles. Aggregation number is defined as the number of surfactant monomers present in the aggregated micelle.

Among other scientists, P. Mukerjee, K. J. Mysels and B. W. Ninham largely contributed with their experimental work on determination of cmc's, distribution of micellar aggregation numbers, and evaluation of cmc determination techniques to the increase of knowledge in the field during the 1960's and 1970's (17, 18).

The number of publications dealing with theoretical models and acquisition of fundamental data continues to increase. Aspects of the present state of the topic will be discussed in later Chapter II, but it can be stated at this point that no generally accepted theory exists that predicts micelle formation and growth in an unambiguous way.

APPLICATIONS OF SURFACTANTS

Besides being still a "hot" topic of current research, micelles pose practical challenges. Micelles are in widespread use in research, industry, and daily life. Probably the most remarkable property of micelles is their ability to solubilize otherwise water-insoluble compounds in their hydrophobic core. This explains the industrial importance of micelles in detergents, cosmetic products, and in emulsion polymerization. In biological systems, lecithin and other phospholipids solubilize cholesterol, and hydrophobic proteins, forming membranes. Certain amphiphiles, such as biological phospholipids, form aggregates called

vesicles or liposomes which can be envisioned as closed, single-, or multilamellar concentric sphere. These are helpful as membrane models or drug carriers.

The following survey is an excerpt of some the most interesting and important applications of amphiphiles, and is by no means complete.

Research Applications

Surfactants find various use in research laboratories mainly due to their useful solubilization properties which can enhance reaction rates and in special cases also enhance the stereoselectivity of a chemical reaction. More specialized applications such as isotope enrichment by micellar photochemistry (19) and the more explicitly discussed examples should provide an insight in this area.

Molecular Weight Determination of Polypeptides. Sodium n-dodecylsulfate (SDS) is nowadays used in a routine biochemical laboratory technique called sodium n-dodecylsulfate polyacrylamide gel electrophoresis (SDS-PAGE). This method allows estimation of the molecular weight of individual polypeptide chains. Under reducing conditions disulfide bonds in the protein are cleaved and SDS unfolds the polypeptide chain by association of its hydrophobic tail with the apolar parts of the polypeptides in a quantitative relation to the chain length of the polypeptide. Each associated SDS molecule adds a negative charge. Performing the electrophoresis along with known protein standards reveals the molecular weight of the tested polypetide chains.

Crystallization of Proteins. Amphiphiles play a practical role in membrane proteins. Due to the amphiphilic nature of the protein itself, it is often impossible to dissolve the protein in aqueous buffers or organic solvents. Micelles can take up membrane proteins in solution by shielding the hydrophobic surface portion from contact water. In 1988 J. Deisenhofer, H. Michel and R. Huber received the Nobel prize for preparation of 3-dimensional crystals and solving the X-ray 3-dimensional crystal structure of

bacteriorhodopsin (20, 21). Bacteriorhodopsin is an integral membrane protein acting as a light energy converting system. The choice of the right surfactant system was the breakthrough in their effort to obtain 3-dimensional crystals. A recent review by M. N. Jones deals in general with the interaction of surfactants with biomembranes and proteins (22).

Solar Energy Conversion and Model Membranes. Photoionization of molecules in micelle and vesicle assemblies is a model system for the storage of light energy (23, 24). Besides the need to construct simple models for biological systems to help to develop and evaluate theories about the structure and function of the photosynthetic apparatus, this research could lead to commercially applicable photo cells (25).

Since biological membranes are often too complex to study, vesicle forming surfactants are welcome model membranes (26, 27). Their physico-chemical properties, such as incorporation of membrane proteins or as drug carrier and delivery systems, are subjects of research probing the questions of structure (28), molecular motion (29), and permeability (30) of membranes, both artificial and biological.

Commercial Applications

The major applications of surfactants in industry or as consumer goods are in cleaning, emulsion polymerization, agricultural crop applications, leather processing, electroplating, petroleum recovery, paper manufacturing, food and beverage additives, pharmaceuticals, photographic products, pigment dispersing agents in paints, adhesives, cement additives, cosmetics, soaps, shampoos, and creams. This list could be extended considerably. For a detailed discussion, recently published books (31, 32) provide a good overview. Only a selection is provided here.

Soaps and Detergents. Soaps and detergents represent the most important economic use of surfactants. In 1984 the worldwide production of soaps and detergents was 24,355,900

metric tons (33). The name soap refers to the alkali salts of natural fatty acids, historically the product of saponification of natural fats and oils. Pouring such huge amounts of surfactants into streams and rivers has of course an impact on the environment. Already in the mid 1950's studies were done on surfactant biodegration, which can be defined as a removal or destruction of chemicals by living organisms. A summary of this extensive research is provided by R. D. Swisher (34). In general biodegration mainly depends on the hydrophobic group. Highly branched surfactants, especially at the alkyl terminus inhibits biodegration. The hydrophilic head group seems to play a minor role.

Emulsion polymerization. Emulsion polymerization is one of the most widely employed polymerization techniques (35, 36). Higher polymer molecular weight and control of reaction rate are the main advantages over polymerizations in bulk or solution. Besides those preferable properties, the reaction mixture has a low viscosity, good temperature control and the removal of unreacted monomer is not complicated. The proposed role of the surfactant is first to form droplets of monomer and initiator. After the reaction is started the micelles stabilize the growing polymer until all monomer is used up. Ideally one reactive growing chain is initiated per micelle, excluding termination reactions.

Micellar Catalysis. It is generally accepted that the rate of chemical reactions depends, among other factors, on the choice of the solvent. Rate enhancements as high as 10^5 have been reported (37), which indicates the commercial potential of micellar catalysis. Since the catalytic effect is based on the stabilization of transition states, reactions carried out in micellar systems can be catalyzed by two proposed mechanisms (37):

a. A micelle can be viewed as a transition zone or gradient between a polar aqueous environment and a nonpolar hydrophobic region, which can be the micellar core or the bulk phase. Hence the micelle represents a reaction chamber of intermediate polarity suitable for stabilizing intermediates.

b. The simple fact that a micellar system can solubilize reactants which would otherwise not be readily available for the reaction is another important criteria. Thus a species might be in very large concentration within a small volume, leading to a large rate enhancement.

Interestingly, micellar catalyses in nonaqueous solvents has gained more and more attention, especially as models for enzymatic reactions (38). The fact that the formation of reverse micelles builds a hydrophilic interior pool, in which water is trapped. Polar substrates are soluble in this pool and a hydrophobic outer shell that can orient nonpolar parts of the reactant can create a system which is specific to a certain functionality resembling enzymatic activity. Reverse micelles serve as hosts for proteins without denaturing them (39). This property is as well of research as of biotechnological interest.

Research in catalytic properties of micellar solvent systems continues to grow. This is because of its practical significance for industrial processes, and the possibility of elucidating reaction mechanisms.

BEHAVIOR OF SURFACTANTS IN SOLUTION

Cmc, Krafft Temperature, and Cloud Point

Probably the most striking observation about amphiphiles is their change of various properties with increasing concentration, shown in Figure 3 (40).

The shown properties are only a selection of the various parameters that change in solution by adding surfactant. Change of the NMR chemical shifts, increased solubility of otherwise insoluble molecules such as benzene and various dyes, enhanced reactivity, self-diffusion, sound velocity, light scattering, and ultracentrifugal sedimentation are further characteristics of surfactants that also show concentration-dependent discontinuities in solution. The concentration region in which those property changes occur (shaded bar in Figure 3) is the critical micelle concentration (cmc). Figure 3 shows that an individual

technique will produce an 'accurate' numerical value, but depending on the choice of method and physical or chemical property to measure one obtains a spread of 'accurate' numerical values which can even differ by one order of magnitude (41). Murkerjee and Mysels (17) discussed 71 different methods to determine the cmc.

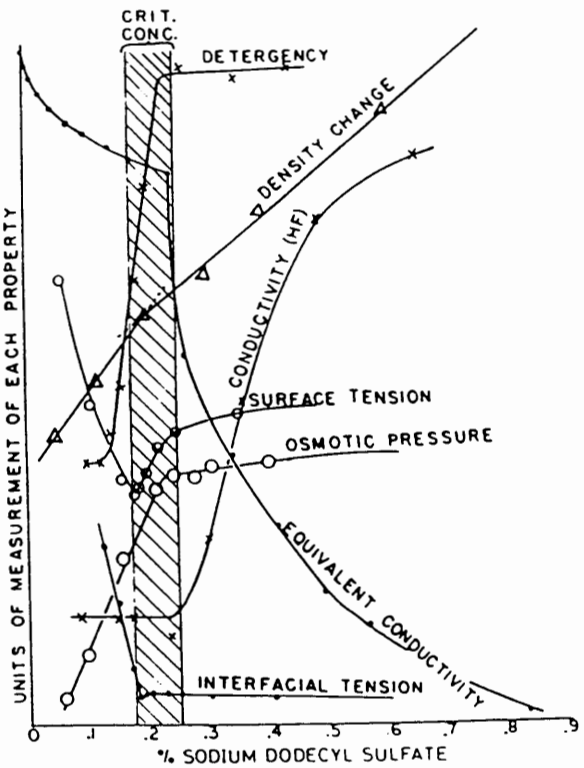

Figure 3. Properties of SDS in solution.

The shown properties are only a selection of the various parameters that change in solution by adding surfactant. Change of the NMR chemical shifts, increased solubility of otherwise insoluble molecules such as benzene and various dyes, enhanced reactivity, self-diffusion, sound velocity, light scattering, and ultracentrifugal sedimentation are further characteristics of surfactants that also show concentration-dependent discontinuities in solution. The concentration region in which those property changes occur (shaded bar in Figure 3) is the critical micelle concentration (cmc). Figure 3 shows that an individual

technique will produce an 'accurate' numerical value, but depending on the choice of method and physical or chemical property to measure one obtains a spread of 'accurate' numerical values which can even differ by one order of magnitude (41). Murkerjee and Mysels (17) discussed 71 different methods to determine the cmc.

Due to the fact that micelle formation is a delicate balance between attractive and repulsive forces, conditions such as temperature, pH, ionic strength of the solution, addition of organic compounds, and pressure can significantly influence the system (42). For instance, many ionic surfactants show enhanced solubility in water upon heating.

Some amphiphiles exhibit a sharp and discontinuous solubility increase at a defined temperature refered to as the Krafft temperature, T_k. For nonionic surfactants, such discontinuous solubility/temperature behavior, although of different nature, is defined as the cloud point. The increase of the temperature decreases the solubility and finally leads to a phase separation.

Variation of the Cmc with Chemical Structure

Hydrocarbon Chain. A major factor determining the cmc is the length of the hydrocarbon chain (42). Experiments show that the cmc decreases logarithmically as the number of carbons increase in a homologous series of surfactants. The mathematical expression (43),

$$\log_{10} \text{cmc} = A - B\, n_c, \qquad (1)$$

contains two substance specific constants A, B, and the number of carbon atoms n_c. Generally, branching or introduction of a double bond causes an increase of the cmc in comparison to the n-alkyl surfactant. Addition of a benzene ring lowers the cmc equivalent to what would be expected for an additional 3.5 methylene groups.

Fluorocarbon Chains. Partly or fully fluorinated carbon chains exhibit significant influence on the cmc compared to the corresponding hydrocarbon (44). While

perfluorinated surfactants have a much lower cmc than the nonfluorinated surfactant, partial fluorination increases the cmc (45).

Head Group. The effect of the hydrophilic head group on micellization depends mostly on its charge and position rather than its shape. In general, a nonionic compound compound has a lower cmc than its ionic equivalent. Additional ionic groups increase the cmc. For example, the cmc of $C_{10}H_{21}CH(COOK)_2$ is 0.13 M while it is 0.024 M for $C_{11}H_{23}COOK$ (46). If the polar group is not positioned at the beginning of the hydrocarbon chain, the cmc decreases.

Counter Ion. The valency of the counter ion plays a major role effecting the cmc. Di- or trivalent ions lower the cmc drastically, although in many cases precipitation occurs. Long chain carboxylates have a low solubility with di- or trivalent cations and do precipitate. It was found (47) that for a given anionic surfactant the cmc decreases in the order of $Li^+ > Na^+ > K^+ > Cs^+ > N(CH_3)_4^+ > N(CH_2CH_3)_4^+ > Ca^{2+} \approx Mg^{2+}$ and for a given cationic surfactant in the order of $F^- > Cl^- > Br^- > NO_3^- > I^-$. Ion pairing generally increases as the counter ion becomes more polarizable and its valency increases. A larger radius of hydration will separate further the ion from the counter ion apart.

Theoretical Models of Micelle Formation

Despite the extensive research done there is no single theory or model of micelle formation, which explains all experimental data and related phenomena, e.g., micellar growth (48). Even the exact nature of the attractive interaction remains unclear. Recent results favor London-dispersion interactions (48, 49) over the release of structural water from the hydrophobic chain (50), which was believed to be the major driving force of aggregation. In any case the reduction of the free energy of the system might be itself a complex process rather than a single step as indicated in Figure 4 (51), illustrating the complexity of surfactant solutions.

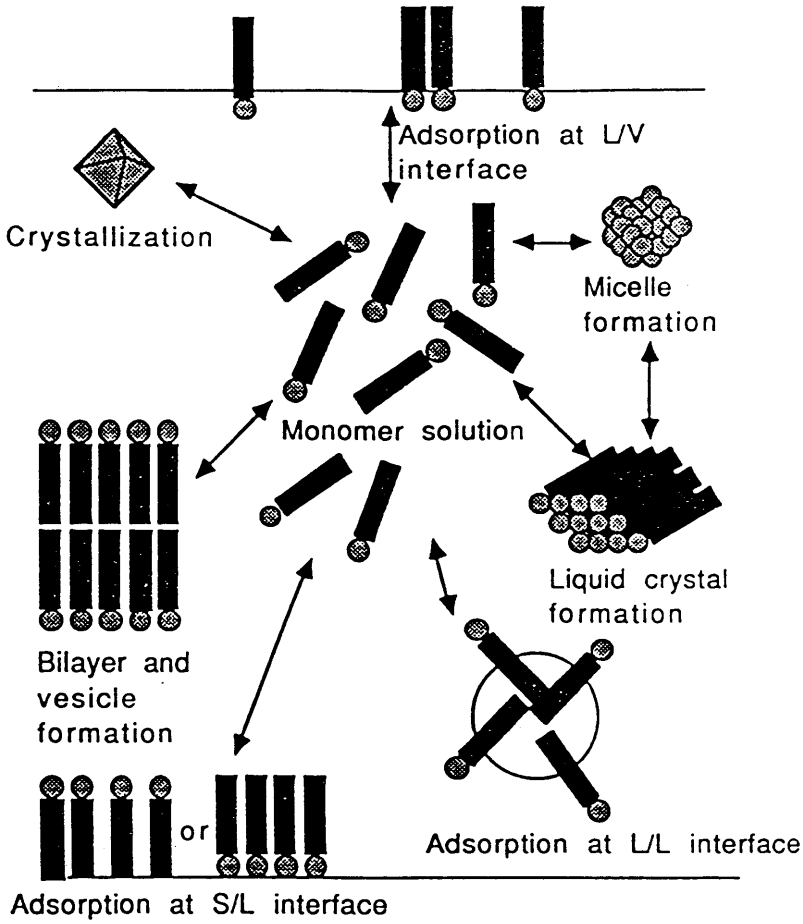

Figure 4. Modes of surfactant action for the reduction of surface and interfacial energies.

To describe the complex behavior, two general approaches are possible: Starting with basic statistical mechanics based on surfactant-water, surfactant-surfactant, and solvent-solvent interactions (52), continuing by correlating those forces on a molecular level and finally trying to come up with satisfactory results this approach has severe pitfalls. As mentioned the exact nature of the attractive forces is still unclear. This fact poses problems in creating meaningful assumptions besides the complexity of the resulting mathematics. This therefore does not seem to be a promising approach yet.

The second approach is to neglect individual forces, but rather to treat the overall thermodynamics of the system. This is now more successful in producing useful (not

necessarily accurate) models (48, 53 - 57). Within these approaches three thermodynamic treatments will be discussed here: the mass-action model, the phase separation model, and the use of molecular geometry to predict micellization behavior, as proposed by Tanford (53) and extended by Israelachivili (58). The basic considerations of predominant models are outlined below. An in-depth discussion is given in reference 57.

Mass-Action Model. The basic assumption of the mass-action model is the existence of an equilibrium between surfactant monomers and the micelle (57). From this assumption it can be stated for nonionic or unionized surfactants,

$$n\ S\ (\text{monomers}) \rightarrow M\ (\text{micelle}). \qquad (2)$$

An equilibrium constant K_M can be formulated,

$$K_M = [M]/[S]^n, \qquad (3)$$

where n is the aggregation number. This simple approach leads to the standard free energy of micelle formation for surfactant molecules,

$$\Delta G_M = R\ T/n\ \{n\ \ln[S] - \ln[M]\}. \qquad (4)$$

The derivation of a similar expression for ionic surfactants is more complicated, because the degree of association of monomer and micelle with the counter ion must be taken into account. Assuming a fully ionized surfactant, one obtains a simple relation,

$$\Delta G_M = R\ T\ (1 + m/n)\ \ln cmc, \qquad (5)$$

where m is the number of counter ions.

Phase Separation or Pseudo-Phase Model. In this approach the micelle is treated as a separate but soluble phase. The cmc is taken to be the saturation limit for the surfactant monomer. Above this concentration there should be no increase of the monomer concentration. Experimentally this is supported by the fact that for many surfactant systems the surface tension remains constant above a certain concentration (54). The Gibbs equation relates the change in the surface tension of a solution, γ, to the surface excess, Γ_2, of surfactant and the free surfactant concentration, [S]. The result is,

$$- d\gamma = \Gamma_2 \, RT \, d \ln[S]. \qquad (6)$$

When the physical property remains constant ($d\gamma = 0$), it must be that [S] does not change, because [S] is constant above the cmc. To obtain thermodynamic parameters from the phase separation model it is necessary to introduce standard states for the system of interest. Defining the standard state of the chemical potential of the micellar and nonmicellar state leads to following expression for nonionic systems,

$$\Delta G_M = RT \, (\ln \text{cmc} - \ln w), \qquad (7)$$

where w is the molar concentration of water (55.4 moles/liter at 20°C). The same considerations apply for ionic surfactants as for the mass-action model.

One drawback to this model is the fact that some surfactants exhibit increased activity above their cmc, which should ideally not be the case. The 'all or nothing' character of micelle formation in the mass-action model is doubtful if not incorrect. Recent calculations suggest (59) that even at low concentration a distribution of premicelles rather than monomers exist in solution. It is also difficult for this approach to address questions such as micellar growth and transitions between aggregation modes.

Tanford's Hydrophobic Effect Approach. Tanford's treatment of micelle formation (53) is based on overall thermodynamic considerations, concluding that the hydrophobic effect (i.e., the release of structured water) is the major driving force of micellization. This hypothesis finds support by the fact that ΔH° of micellar formation for almost all surfactants is small or positive (60), whereas ΔG° is negative. Hence ΔS° must positive and large, and micelle formation is a entropy-driven process in water. The Tanford model also applies to membranes, and proteins addressing questions such as ligand binding, conformation, and conformational changes and protein folding. Extending Tanford's theory, Isrealachvili used the geometric and packing properties of the individual surfactant to predict and explain the overall geometry and stability of the resulting aggregates. The

practicality and elegance of his work by introducing a critical packing parameter is shown in Figure 5 (61).

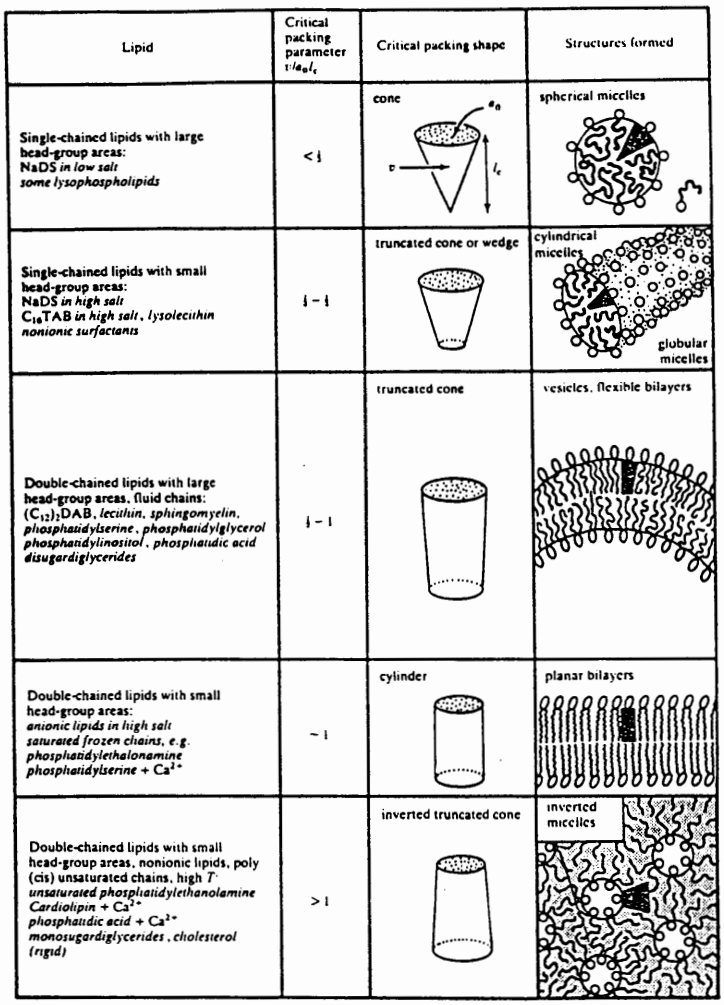

Figure 5. Dynamic packing properties of lipids and the structure they form.

Size, Shape, and Structure of Micelles

To address questions such as size, shape, and structures of micelles, the application of spectroscopic techniques becomes crucial. Among various options such as light scattering techniques (62), (e.g. neutron diffraction, quasi-elastic light scattering, photon correlation spectroscopy), fluorescence, and positron annihilation techniques, NMR proves to very successful in application to surfactant solutions (63). The range of information that can be

obtained starts at the submolecular level, allowing studies on conformational and dynamic properties of the amphiphile, and reaches to the macroscopic level, where questions such as diffusion and determination of phase diagrams can be answered. The advantage of being a noninvasive solution state method allows studies without disturbing the equilibrium state. Various nuclei can reveal different kinds of information. ^{1}H, ^{2}H, ^{13}C, ^{19}F, ^{17}O, ^{14}N, ^{31}P, ^{7}Li, and ^{23}Na represent some of the most important nuclei studied by NMR. Especially from quadropoles (^{2}H) important insights in geometry can be obtained from the orientation dependence of the nuclei vs the applied magnetic field (64). A detailed discussion about NMR and surfactant solution is given in later.

Light scattering techniques are particularly powerful for determining the size and shape of micelles. Although the classical micellar shape is considered to be a sphere, this simple picture does not reflect experimental truth, and might be in fact the exception. Examples of five predominant micellar shapes are given in Figure 6 (65).

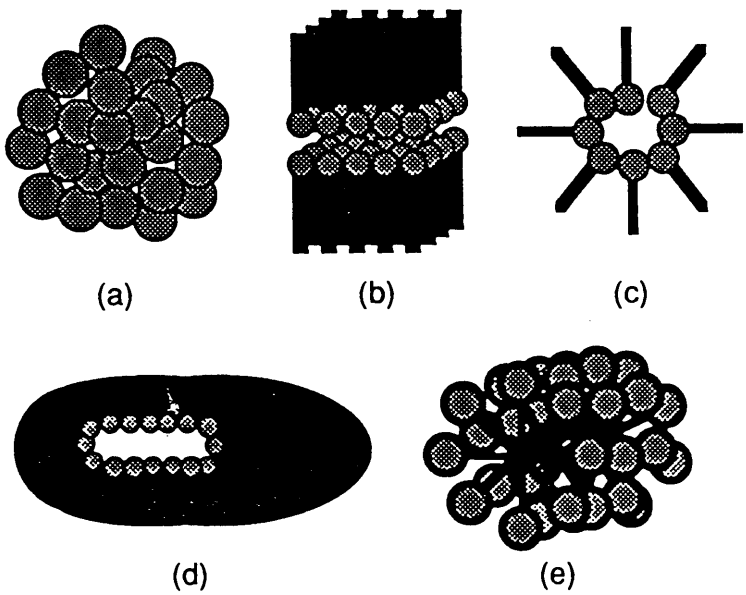

Figure 6. Illustration of five important micelle shapes, as interpreted from experimental data: a) spherical, b) lamellar, c) inverted, d) disk e) cylindrical or rod.

Size. The aggregate number may vary considerably between the different shapes, typically from as low as 20 up to 200. Aggregation numbers of 7500 and higher are known (66). As already mentioned, a traditional technique for determining aggregation numbers was introduced by Debye. Newer methods use laser light scattering (67) or fluorescence quenching (68). A typical diameter for a spherical micelle is around 2.5 nm but 20 - 50 nm for small and 100 - 1000 nm for large unilamellar vesicles. Since micelles are highly dynamic systems, the picture of a smooth surface is oversimplified and must be rather viewed as a time averaged picture. If one could take a 'snapshot' of a micelle one would see an irregular surface. There is also evidence that micelles appear in a distribution of aggregate sizes and even shapes (69).

Shapes. Figure 4, 5, and 6 show different possible shapes of micelles and the structural characteristics of the surfactant molecule leading to the individual structure. It must be pointed out that in solution transitions between different shapes are common (70) depending mostly on concentration of the surfactant but also on temperature and other parameters.

Structure. The internal structure of micelles is still under scientific discourse, although there is general agreement on certain points. The interior of a micelle is represented in Figure 7 (71), 8, and 9.

The micelle is assumed to be in aqueous solution. The hydrocarbon chains pack at liquid-hydrocarbon density in the core. Each segment of the individual hydrocarbon chain spends a considerable time close to the surface of the micelle (see Figure 7 and 9). Although the core of the micelle is almost completely expelled from water, every segment experiences a hydrophilic environment. The depth in the micelle of each chain segment is based on calculations of Gruen and Lacey (72). Kinetic aspects of this model are discussed in the next section.

The fact that the hydrophobic chains are not simply straight in a micelle has been quantified by Dill and Flory. Their proposed lattice model of a spherical micelle is presented in Figu 3).

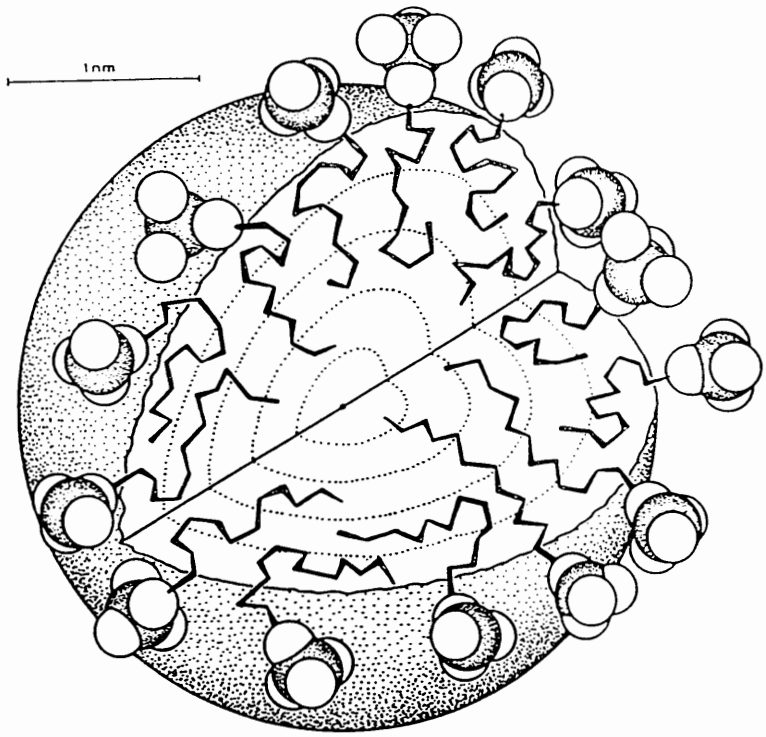

Figure 7. A sodium dodecylsulfate (SDS) micelle drawn to scale.

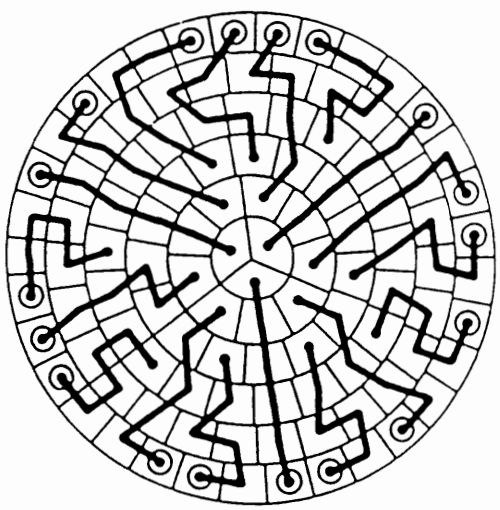

Figure 8. Lattice model of a spherical micelle.

The sphere is partitioned in parts of equal size and the chains are positioned in such a manner that no field is occupied twice. The first chains are put in straight, so that the inner core is occupied. Positioning of the later chains obeys the rule, that no space can be occupied twice leads to the proposed structure of Figure 8.

Although it is generally accepted that water is mostly excluded from the hydrophobic core, recent articles (74) indicate that water penetration in SDS micelles at 25°C does exist. Extensive ^{19}F NMR studies had been made to study water penetration of micelles in dependence of increased temperature (75). ^{17}O (76) and multi-dimensional NMR studies (77, 78) are promising tools for approaching the subject.

Internal Motion and Self Diffusion of Micelles. Again, NMR proves to be useful in exploring the effect of micellization on the molecular motion of the amphiphile. Especially ^{13}C spin-lattice relaxation time (T_1) studies on each individual carbon of the hydrocarbon chain revealed (79, 80) that the internal motions of the molecule are hardly effected by micellization as the methyl end of the hydrocarbon chain is approached. The C_1 carbon, which is the closest to the head group, finds its ability to rotate decreased by roughly one order of magnitude in comparison to the monomeric system. The interior of a micelle is said to be fluidlike because no evidence for an ordered structure is found as the inner core of the micelle is approached. Therefore the "tails" resemble the liquid state. An illustration of the flexibility of an 8-carbons surfactant in its micellar state is given in Figure 9 (81). The data which was derived by Chevalier and coworkers shows that the mobility increases from the hydrophilic head to the hydrophobic end of the molecule. Molecular tumbling of the whole amphiphile is restricted because of incorporation in the micellar structure.

The question of diffusion is typically addressed by light scattering methods (62), although recent developments and improvements of magnetic field gradient techniques expands NMR applications into this area. Scattering techniques cover size ranges from a few nanometers up to some microns. The diffusion coefficient is determined in light

scattering methods by the frequency shift of the scattered coherent laser light. The diffusion coefficient is actually used to relate to an equivalent hydrodynamic radius. The ability to study mixtures of different surfactants is not possible for light-scattering techniques.

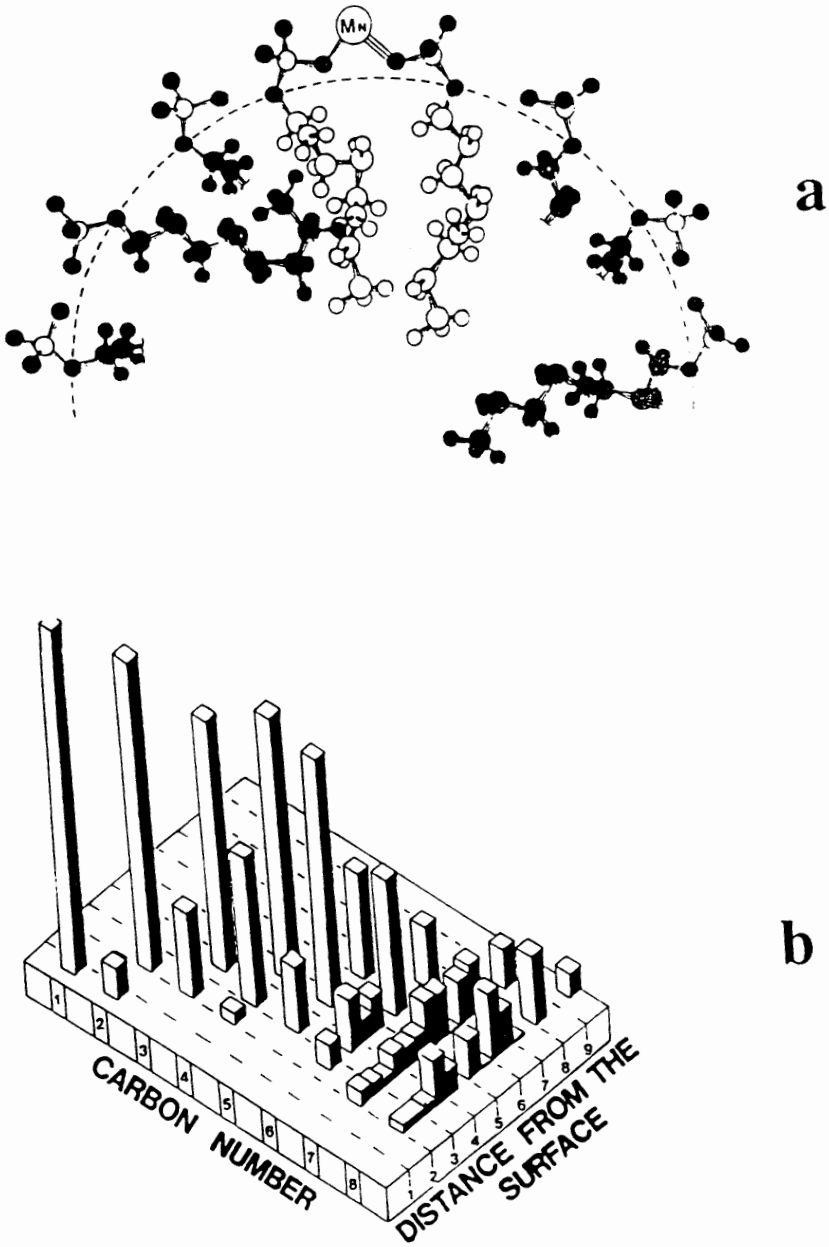

Figure 9. Mobility in a micellar system. In part a), Mn^{2+} is binding at the surface of a monooctyl hydrogenophosphate micelle. Part b) shows the probability distributions of distances of the chain carbons to the micellar surface normalized to carbon 1.

Diffusion-ordered two-dimensional NMR spectroscopy (DOSY) is able to identify molecular components of mixtures and simultaneously characterize the size of the aggregates or the diffusion coefficients (82). The diffusion coefficient value depends on the micellar shape, and size and, is around $5.54 \cdot 10^{-7}$ cm^2/sec for mixed micelles of 4 mM SDS and 8 mM octaethylene glycol dodecyl ether, and $1.86 \cdot 10^{-8}$ cm^2/sec for unilamellar vesicals of 100 mM 1-palmitoyl-2-oleoyl phosphatidylcholine; the value for free water is $1.2 \cdot 10^{-5}$ cm^2/sec.

NMR OF MICELLAR SYSTEMS

The application of NMR to micellar systems started to become popular after commercial Fourier transform (FT) NMR spectrometers became available. Therefore the number of publications each year was only about ten until the early 1970's.

The range of applications and accessible nuclei was briefly pointed out in the previous sections and will not be discussed in this text, but recent reviews provide a good overview (83, 84). Besides the already stated advantages of NMR over other techniques, NMR's sensitivity to solute-solvent interactions. The fact that dynamic information can be obtained in addition to structural information leads to the next section, which deals exclusively with dynamic aspects of NMR.

Dynamic Nuclear Magnetic Resonance (DNMR)

Since NMR is a solution state method, the obtained signal contains information about the motions of the measured nuclei. DNMR can be defined as the effect of chemical exchange processes on a NMR spectrum. A comprehensive review of reaction kinetics and exchange, with various references, was published recently (85). Caused by changes of the environment of the magnetic nuclei, the NMR spectrum may exhibit different chemical shifts and/or coupling constants for each of the sites in which the nuclei reside. The most

valuable information that can be obtained is the rate constant, k, for the exchanging system. It is important to introduce at this point the concept of the "NMR time scale", which is defined as the time domain of exchange giving rise to dramatic changes in NMR spectra and/or NMR measurable parameters. The lifetime under conditions that cause the signals for exchanging species to just coalesce into a single signal for a two site exchange situation is defined as:

$$\tau_{coal} = \sqrt{2}\ (\pi\ \Delta\nu)^{-1} = k^{-1} \qquad (8)$$

where τ_{coal} is the coalescence lifetime given in seconds and $\Delta\nu$ the chemical shift difference between A and B in Hz, which depends on the magnetic field of the spectrometer. The magnetic field is refered to the resonance frequency of protons, e.g. 400 MHz at 9.4 Tesla.

For example, a two-site exchange of the methyl protons in N,N-dimethylformamide has a coalescence lifetime of ≈ 30 ms at 60 MHz magnetic field strength, but at 400 MHz a τ_{coal} of ≈ 5 ms. The coalescence lifetime marks the transition from a "slow" process to a "fast" process on the "NMR time scale". Since the value depends strongly on the magnetic field strength of the spectrometer, it is less ambiguous to state that a process is "fast" or "slow" on the "chemical shift time scale" if reasoned in Hz.

The NMR chemical shift time domain ranges from a few picoseconds to more than seconds if the sample can be carefully thermostated. In other words, a range of many orders of magnitude can be studied with the same instrument by a variety of experiments. This incredible range shows the flexibility of NMR. To study chemical exchange processes different NMR techniques are possible. The choice of the method depends on the characteristics of the system to be studied. Among the most important techniques are saturation transfer, selective pulse transfer, and 2D exchange spectroscopy (2D EXSY, also known as nuclear Overhauser effect spectroscopy, or NOESY because it employs the same pulse sequence), and the complete bandshape (CBS) method. The CBS method proves to be the most accurate technique if the system is close to τ_{coal}. This can be crucial

because a comparison of results for the mentioned techniques performed on the same system (86) shows that the measured rate constants can differ by as much as 40%.

The carbamates were chosen for this study for the very reason that their N-methyl peak is close τ_{coal} within the temperature range between 0°C and 100°C, so that water can be used as the solvent. The analogous amides show such behavior only above the boiling point of water. Therefore the CBS method is discussed in greater detail next. The treatment of theory and its application is obtained from Sandström's book (87) and the references cited within.

The CBS Method. Unlike other methods used to analyze the 1D NMR spectrum, the CBS method is based on reproducing the measured signal by a calculated one. Other techniques simply measure one parameter of the NMR signal such as the width at half maximum of the peak, ratio of the maximum intensity of peak A and B, or the separation of the peaks and relate them to the exchange rate with limiting assumptions. All those techniques allow an immediate estimate of the exchange rate but do not produce data as accurate as the CBS method. The CBS method takes various parameters into account, and does not depend on measuring any one to a high precession. It is a trial and error technique which can be performed by visual comparison of the measured and calculated peak.
The N-methyl peak of the carbamates represents a typical two-site exchange problem. No indication of a third conformation was ever found. The transfer of the methyl protons from site A to site B can be assumed to be first order. By introducing these assumptions one obtains the modified Bloch equations:

$$dG_A/dt = -\alpha_A G_A - iC_A - k_A G_A + k_B G_B \qquad (9)$$

$$dG_B/dt = -\alpha_B G_B - iC_B - k_B G_B + k_A G_A \qquad (10)$$

where G_A and G_B are the complex magnetic moments in site A and B, α is the spin wave function with spin 1/2, and k_A and k_B are the rate constants for interconvertion from site A to B). Solving these modified Bloch equations leads to an expression for slow passage

conditions which gives the bandshape as a function of the exchange rate (k_A), the population of peak A (P_A), the chemical shift separation (dv), and the transverse relaxation times for peak A and B (T_{2A}, T_{2B}). An example of the obtained spectra of an N-methyl peak of NaOcSarc at 172 mM at various temperatures and the calculated bandshape fits are presented in Figure 10. This Figure illustrates the quality of the calculated linefit to the actual measured NMR signal. It should be pointed out that these fits reach the digital resolution of the spectra. An illustration of the most characteristic cases is provided in Figure 10. At 298 K the ^1H NMR signal of the N-methyl peak is slow on the chemical shift time scale and two separated peaks for the two conformations can be seen. The generated bandshape reveals a peak A (the major peak) lifetime of 0.58 sec. Increasing the temperature to 313 K, and finally to 338 K changes significantly the appearance of the signal. The peaks coalesce and finally give only rise to a single peak. The most sensitive linefit is around τ_{coal}, where small changes in the third significant figure of τ alter considerably the outcome of the computed signal. The situation is less favorable at the extreme high and low temperature cases.

Once the exchange rate is determined, the corresponding activation parameters can be determined graphically using Equations 11 and 12. Activation parameters $\Delta G^{\ddagger}$, $\Delta H^{\ddagger}$, and $\Delta S^{\ddagger}$ for rotation about the C-N bond are obtained by using the experimentally determined $\tau = k^{-1}$ by applying the following equations from Eyring's absolute rate theory, relating the rate of a process to its activation barrier (11):

$$\Delta G^{\ddagger} = aT\,[10.319 + \log (T/k)] \qquad (11)$$

$$\log(k/T) = -\Delta H^{\ddagger}/aT + \Delta S^{\ddagger}/a + 10.319 \qquad (12)$$

Here, $a = 4.575 \cdot 10^{-3}$, which gives $\Delta G^{\ddagger}$ $\Delta H^{\ddagger}$ in kcal/mol, and $\Delta S^{\ddagger}$ in eu, T = temperature in K, and k is the rate constant, in Hz (s^{-1}).

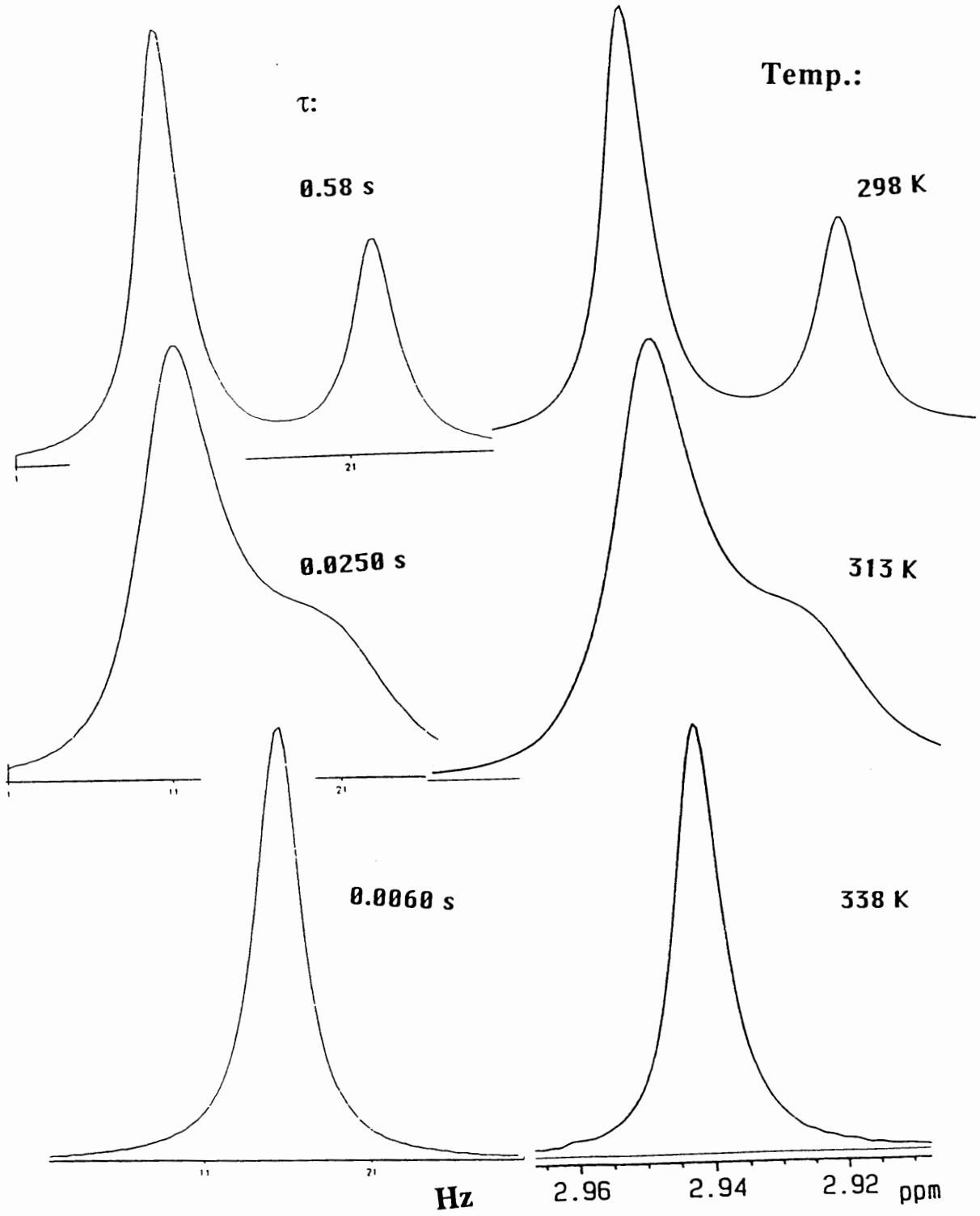

Figure 10. Comparison of the computed bandshape (left) to the measured N-methyl signal (right) of NaOcSarc in its micellar state.

CHAPTER III

EXPERIMENTAL PROCEDURES

SYNTHESIS

Synthesis of Sodium N-(octyloxycarbonyl)sarcosinate (NaOcSarc)

The basic procedure of Gerig et al. (8) was followed. Sarcosine hydrochloride (0.33 g = 2.6 mmol) was dissolved in 1.7 mL 20% dioxane in water and the solution was adjusted to pH 10 with concentrated NaOH. The reaction mixture was cooled with an ice bath and stirred magnetically. Octylchloroformate (0.51 mL = 2.6 mmol) was added dropwise. The mixture was stirred for 2.5 h, acidified to pH 1.8 with concentrated HCl and extracted 4 times with a total of 8 mL chloroform. The organic phase was dried overnight over sodium sulfate. The chloroform was removed on a rotary evaporator. The residue (a viscous liquid) was dissolved in hot cyclohexane, filtered through paper and titrated with 0.1 N NaOH until all the precipitate was dissolved (pH = 7.5). The aqueous solution was filtered through paper and lyophilized to obtain 0.27 g (39%) of a white powder. The powder was recrystallized 3 times with 95% ethanol and gave a melting point: 73-75°C.

Synthesis of Lithium N-(octyloxycarbonyl)sarcosinate (LiOcSarc)

The lyophilized NaOcSarc was acidified to pH = 2 with concentrated HCl. The solution was extracted 3 times with a total of 12 mL chloroform. The chloroform was removed by rotary evaporation. An oily liquid remained which was dissolved in H_2O and titrated with 0.1 M LiOH to pH = 7.9 and was lyophilized again to obtain a white powder. The melting point is 220°C.

Synthesis of Eicosylchloroformate

The basic procedure of Haas et al (89) was adopted, although it had to be slighlty modfied since first attempts obeying the same conditions did not lead to product. A solution of 20% phosgene in toluene (6.0 mL = 0.012 mol) was heated to 70°C in a 25 mL flask with condenser and stirred magnetically. Eicosanol (0.67 g = 2.2 mmol) was melted and added slowly. After all eicosanol was added the reaction was stirred for additional two hours maintaining the temperature at 70°C. Then the solution was poured over 5 g of crushed ice. The organic top layer was separated from the aqueous layer with a separatory funnel. The organic phase was placed under water pump vacuum for 30 minutes to remove all phosgene.

Synthesis of Sodium N-(eicosyloxycarbonyl)sarcosinate (NaEiSarc)

The basic procedure of Gerig et al (8) was followed. Eicosylchloroformate from the previous synthesis was dissolved in 40 mL toluene. Sarcosine hydrochloride (2.7 = 22 mmol) was dissolved in 5 mL 20% dioxane in water and heated to 55°C. The pH was adjusted to 10 with concentrated NaOH. The sarcosine hydrochloride solution was stirred magnetically and eicosylchloroformate was added dropwise. The pH was kept between 9 - 12 by adding 2 N NaOH. Stirring was continued for 2.5 hours. The solution was acidified with concentrated HCl to pH 2, then extracted 3 times with a total of 25 mL chloroform. The chloroform was removed by rotary evaporating and a white, and waxy compound was titrated with 0.1 M NaOH. A milky dispersion resulted, which was filtered trough paper. The cloudy solution was lyophilized and checked by ^1H NMR. Due to the low solubility in $CDCl_3$ and D_2O even with 1024 scans it remains difficult to identify the characteristic N-methyl peak. Therefore the spectrum is not reported at this point. The filtrate was dissolved in $CDCl_3$ and showed after 32 scans a strong signal in the N-methyl region.

Synthesis of sodium N-(decyloxycarbonyl)sarcosinate (NaDecSarc)

Nine mL of 20% phosgene in toluene (0.0174 mol) were stirred magnetically and cooled with an ice-bath. Dropwise 3.3 mL of decanol (0.0173 mol) were added and stirred for 30 minutes. The temperature was kept between 0-5°C. After 2 hours of stirring, the solution was poured over 38 g of crushed ice. The organic layer was separated from the aqueous one. Sarcosine hydrochloride (1.05g = 8.4 mmol) was dissolved in 10.0 mL of 20% dioxane in water and adjusted to pH 10 with conc. NaOH. The crude decylchloroformate was added dropwise. The reaction was kept between pH 9-11 with 2 M NaOH. After 2 hours of stirring the reaction was allowed to warm up to room temperature. After 3 more hours the reaction was acidified to pH 2 with concentrated HCl and extracted 4 times with a total of 40 mL chloroform. Na_2SO_4 was added to the chloroform and left overnight. The chloroform was removed by rotary evaporation. An oily liquid remained and was dissolved in 15 mL hot cyclohexane and filtered through paper. The solution was mixed with 20 mL water and titrated with 0.1 N NaOH to pH 7.4. The two phases were separated. The aqueous solution was lyophilized to obtain 0.64 g of a white powder (yield = 61%).

The compound was recrystalized from ethanol 3 times to obtain a ^1H NMR spectrum which shows almost no impurities. The melting point was 64-66°C.

Synthesis of 10-nonadecanol

In order to synthesize a 2 stranded long chain carbamate, 10-nonadecanone was reduced to the corresponding alcohol (89, 90). 2.09 g (= 55 mmol) $LiAlH_4$ were dissolved in 70 mL abs. ether and rinsed in a 3-neck 500 mL flask to which a condenser, a $CaCl_2$ tube, a dropping funnel and on the last opening a stopper were adjusted. 10-nonadecanone (14.23 g = 0.05 M) were tried to dissolve in 70 mL abs. ether. Only 2 g of ketone could be dissolved (conc.= 7.0 mM). The saturated ether was placed in the dropping funnel. The

$LiAlH_4$ solution was stirred magnetically and cooled with an ice water bath. The ketone was added dropwise (≈ 15 min.). The reaction was stirred for 6 hours. Carefully ice water was added to the reaction until no bubbles could be seen anymore. Then 10% H_2SO_4 were added until all compound dissolved (≈ 200 mL). The 2 phases were resolved in a separatory funnel and the aqueous phase was treated 3 times with a total of 60 mL abs. ether. The ether phase was treated with saturated KCl solution 3 times with a total of 90 ml. The ether was removed with a rotary evaporator. 1.6 g of white powder were obtained. One recrystalisation from petrol ether was made. Melting point = 60-62°C (Lit.: 65.7-67°C). The ^{1}H-NMR spectrum in chloroform-d showed formed product (H-C-OH peak) but the integrals indicate the presence of ketone. Further recrystalizations are anticipated.

Synthesis of octanoic acid chloride

0.025 mol (Mr: 144) of octanoic acid (≈ 4.45g; ≈ 2.7 mL) and 0.038 mol (Mr: 119) of fresh distilled thionyl chloride (≈ 3.95 g; ≈ 3.95 mL) were heated to 80°C with a condenser in a 25 mL flask until no bubbles could been seen anymore. Unreacted thionyl chloride was distilled (7). The residue was directly taken for the synthesis sodium N-octanoylsarcosinate.

Synthesis of sodium N-octanoylsarcosinate (SNOS)

The slightly yellow product of the previous reaction was taken for this synthesis. Excess of sarcosine hydrochloride (0.03 mol ≈ 3.8 g) was dissolved in water and magnetically stirred. The pH was adjusted to 10 with conc. NaOH. 3 mL (0.016 M) of octanoic acid chloride were added dropwise. The pH was kept between 9-13 with 2 M NaOH. The temperature was kept below 35°C. After 1.5 h the solution was acidified with conc. HCl to pH = 3.5 and was extracted 3 times with a total of 25 mL ether. After the ether was evaporated an oily, colorless fluid remained. After 2 h crystals could been seen. The oily compound and the crystals were taken up with hot cyclohexane. The crystals

could not been dissolved. The cyclohexane was filtered through paper. The filtrate was titrated with 2 N NaOH. From pH ≈ 3 heavy precipitation took place. The precipitation could not be dissolved up to pH = 12. Therefore the pH was adjusted at pH = 8.5 and the mixture was filtered through paper. The resulting solution was lyophilized and 3.2 g of a white powder were obtained (54 %). Only a fraction of it (0.38 g) was recrystallized 3 times in methanol. Melting point: 139-141°C.

Synthesis of HDecSarc and HOcsarc

Both compound were prepared from the corresponding lithium sarcosinates salts by the same procedure. The salt was weighed in on a Mettler (Mettler H20 T) high precision balance. The salt was dissolved in ≈ 20 mL destilled water and titrated with conc. HCl to pH = 2.0. The resulting suspension was washed 3 times with a total of 20 mL chloroform. The organic phase was placed in a flask, and dried overnight over Na_2SO_4. The chloroform was removed by rotary evaporation. To the remaining viscous liquid 500 µL DMSO-d_6 was added. The solution was transfered to a NMR tube with a micro pipette. The later reported concentrations for the NMR temperature studies are based on the assumption, that 100% of the salt was converted to the corresponding acid and quantitatively transfered.

Compound Research

For NaOcSarc, HOcSarc, NaDecSarc, and HDecSarc a Chemical Abstract Service (CBS) Online computer search via Scientific & Technical International Network provided by the American Chemical Society (ACS) was performed at the 9th of november 1992. None of the above mentioned compounds nor any other possible salt with a different counter ion were reported at this point. Therefore no literature melting points are listed.

^{1}H NMR Spectroscopy

^{1}H NMR spectra were generated, on a Bruker AMX FT-NMR spectrometer at 400.14 MHz. A low pulse angle (~30°) was used along with a long repitition rate (~7 sec) to minimize saturation, giving reliable integrals and peak shapes. Spectra were collected as 16K - 64K data sets. Only if the spectrum showed hardly any impurities was the compound used for variable-temperature ^{1}H NMR studies to determine the activation parameters. The ROESY data sets were obtained according to the usual protocol (91).

DETERMINATION OF THE CMC

Since the population ratio of the N-methyl peaks of the synthesized carbamates is mainly concentration dependent, the population ratio of the two peaks was measured at different surfactant concentrations to determine their cmc. For this purpose the previously synthesized salts were weighed on a Mettler H20T balance and dissolved in 510 μL D_2O. The resulting concentration was calculated. The solution (500 μL) was placed in a NMR tube. All further samples were prepared by dilution with D_2O. The pH of the samples was 6.9 and the temperature was 298 K. The population of the N-methyl peaks was determined by integration of the peaks. The cmc's were determined graphically by plotting % population of the downfield signal (P_A) vs concentration of surfactant. The concentration were a significant population change took place is defined as the cmc. The cmc is determined graphically by extrapolation of the obtained data points trying to hit the onset of the population change. To establish the quality of this method the cmc of SNOS was measured by this technique, and compared to the known literature value. The method proved to reproduce the reported value. Also the dependence of the chemical shift of the N-methyl group upon concentration changes was used to determine the cmc of NaOcSarc. Data and results are given in Chapter IV.

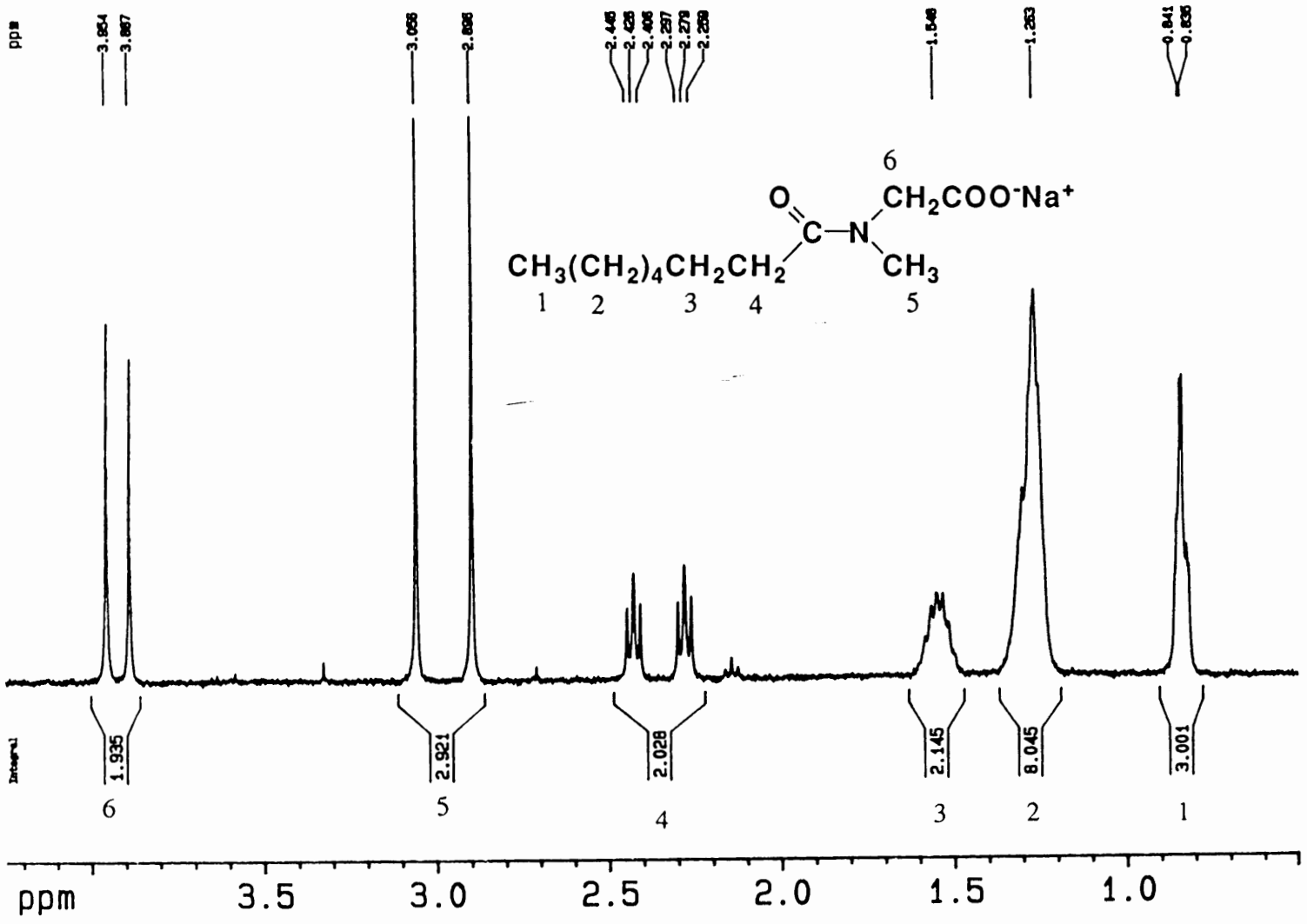

Figure 11. ^{1}H NMR spectrum of SNOS at 298 K, [SNOS] = 2 mM. Assignments of the peaks are based on chemical shifts and integrals

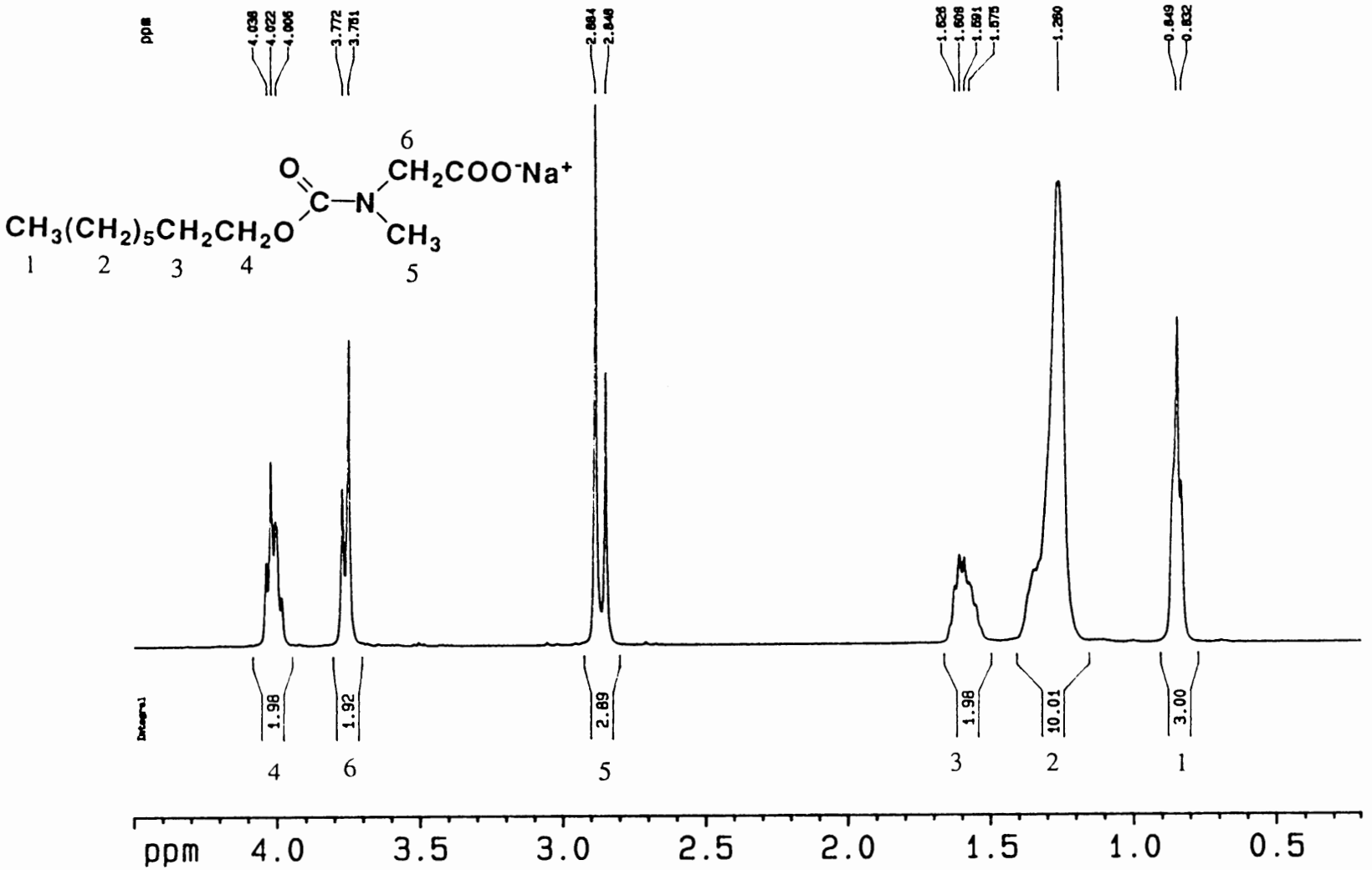

Figure 12. ^{1}H NMR spectrum of LiOcSarc at 298 K, [LiOcSarc] = 270 mM. Assignments are based on chemical shifts and integrals.

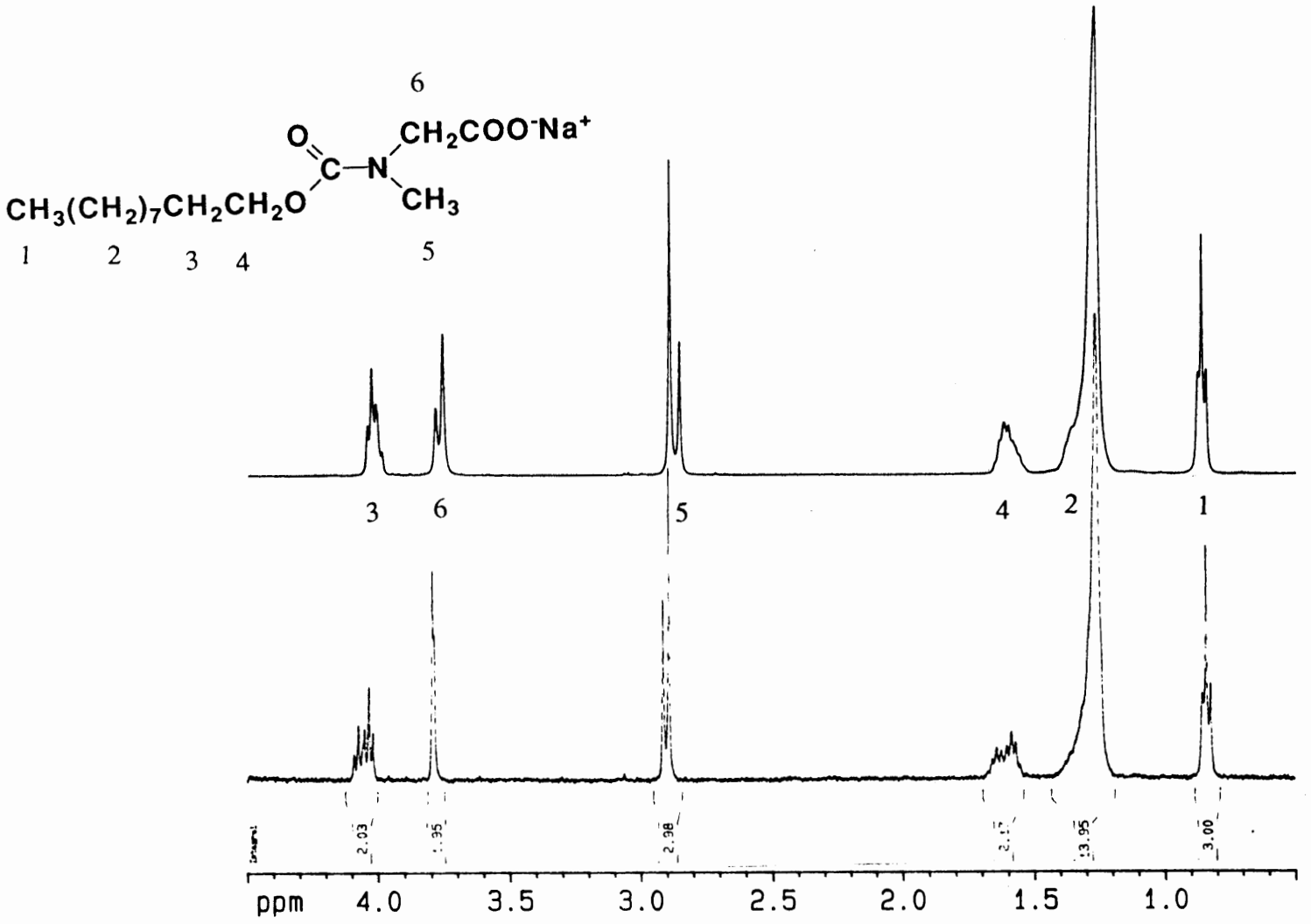

Figure 13. ^{1}H NMR spectrum of NaDecSarc at 298 K, [NaDecSarc] = 0.95 mM in the bottom spectrum, and 116 mM in the top spectrum. The comparison visualizes the effect of surfactant concentration on the spectra. Assignments are based on chemical shifts and integrals.

VARIABLE TEMPERATURE DEPENDENT ^{1}H NMR SPECTRA AND THE COMPLETE BANDSHAPE (CBS) ANALYSIS

The ^{1}H NMR spectra of the various surfactants were obtained from 298 K - 338 K in 5° steps. Systematic errors were minimized by the acquiring the spectra in the following order: The first spectrum was obtained at 298 K the following spectra up to 338 K were acquired in 10 K steps. Then the temperature was lowered to 333 K, continuing to lower the temperature in 10 K steps until 303 K is reached. It was not done in all cases due to simple time constraints. A difference in quality of the data was never noticed. ^{1}H NMR temperature runs which were performed by this sequence are indicated with a '*'. The other systems were studied starting from 298 K, proceeding in 5 K intervals up to 338 K. For some systems the 338 K spectrum could not be obtained due to instrumental problems.

The CBS analysis is based on solving the modified Bloch equations (see introduction p. 24) for an uncoupled two-site exchange case. The program, which was used to calculate the signal, is given in the Appendix, and was run in FORTRAN on a personal computer (Macintosh II). The calculated data points were pasted in a program called Cricket Graph to generate the final signal. The computer calculated signal was visually compared with the measured NMR signal. An example of the quality of the CBS method is given in Figure 10. Especially in the intermediate temperature region, where the two peaks start to coalesce, the bandshape is very sensitive to little changes in τ.

DETERMINATION OF THE ACTIVATION PARAMETERS

The basic set of equations used to calculate the exchange rate (k) was outlined in the introduction part of this thesis. Plotting log(k/T) vs 1/T (Arrhenius plot) lead to the activation parameters from equations 11 and 12. A discussion of reliablity and errors is provided at the end of Chapter IV.

CHAPTER IV

RESULTS

CMC DETERMINATIONS

For determining the cmc of the surfactants a ^1H NMR technique was chosen. The population of the N-methyl peak as well as the chemical shift difference in dependence of surfactant concentration at 298 K and pH = 6.9 were obtained and plotted vs the concentration to determine the cmc.

Cmc of NaOcSarc w/o Salt Addition

The cmc of NaOcSarc is determined by the outlined procedure (p.32)

TABLE I

CONCENTRATION-DEPENDENCE OF P_A OF NaOcSarc W/O SALT ADDITION

[NaOcSarc] (mM)	P_A (%)	[NaOcSarc] (mM)	P_A (%)
172.2	61.0	57.8	42.0
138.6	61.1	46.2	40.5
115.5	56.9	38.5	38.3
86.6	50.8	28.9	37.7
77.7	47.8	14.5	37.8
69.3	45.0	2.9	37.8
63.0	44.1		

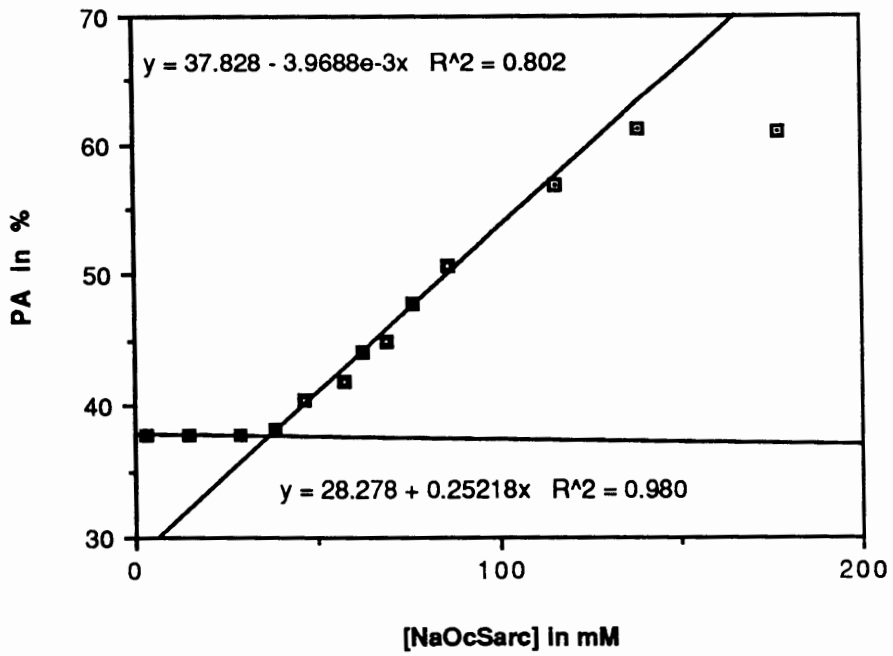

Figure 14. Cmc determination of NaOcSarc.

The cmc is determined by calculating the x-value of the intersection of the two straight lines.This method was employed for all surfactants. A summary of the results in given in Table XVIII. The value of the cmc for NaOcSarc was thus found to be 37 mM.

Cmc of NaOcSarc with Salt Addition

The cmc of NaOcSarc is determined by both the procedure outlined above, and by the concentration-dependence of the N-methyl signal's chemical shift (δ). I first show results for monitoring the relative populations; in this analysis A refers to the further downfield shifted peak, and B to the further upfield peak. Then I show the results for the chemical shift plot. It seems that the results from this second method are more ambiguous. Only the plot of chemical shift differences in peak A are shown.The arrow-indicated x-value is not taken into account. Whether one considers the third highest chemical shift value as part of the low or high concentration set leads to a different cmc result.

TABLE II

CONCENTRATION-DEPENDENCE OF P_A, AND δ OF NaOcSarc WITH 1.06 M NaCl

concentration (M)	P_A (%)	δA (ppm)	δB (ppm)
0.156	72.3	2.984	2.950
0.0779	69.9	2.984	2.954
0.0389	64.7	2.987	2.962
0.0260	55.9	2.987	2.965
0.0195	50.0	2.994	2.973
0.0130	41.5	2.986	2.966
0.00973	41.5	3.004	2.981
0.00649	41.1	3.007	2.982
0.00487	39.4	3.008	2.9483

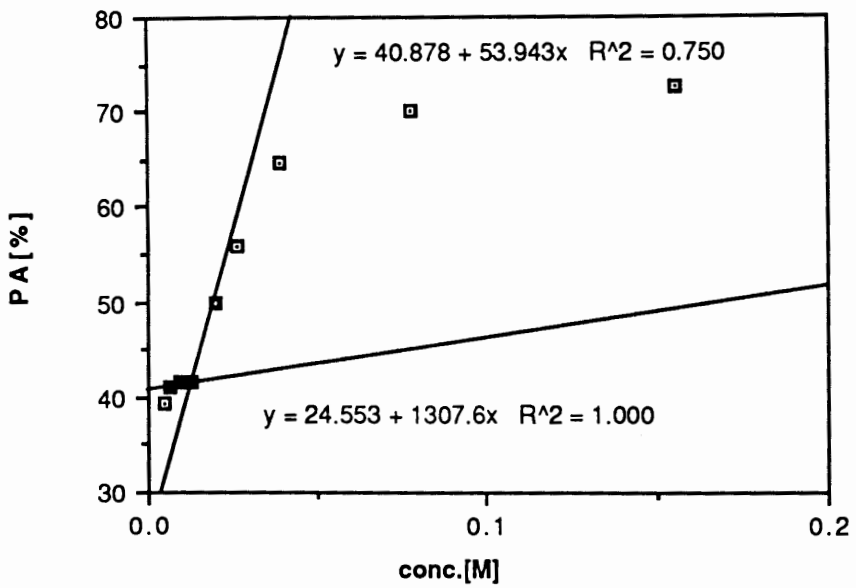

Figure 15. Cmc determination of NaOcSarc with 1.06 M NaCl; cmc = 0.013 M.

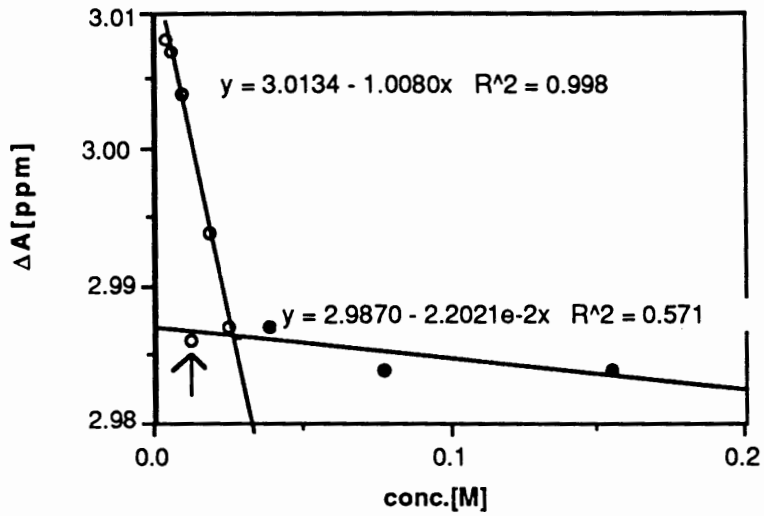

Figure 16. Cmc determination of NaOcSarc with 1.06 M NaCl; cmc = 0.027 M. Data for the change in chemical shift of peak B is not shown.

These data support the previously determined cmc and give an idea about the error. The method of choice remains the concentration dependency of P_A because the changes are significant and easy to measure. The change of the chemical shift is in a rather small range (0.03 ppm). Consequently it must be measured to high precision in order to obtain reliable data. The poplution ratio does not depend so extremly on a high precision measurement which makes it less vulnerable to measurement errors. A detailed discussion of error is provided at the of this Chapter.

Cmc of LiOcSarc w/o Salt Addition

Although the starting solution showed cloudiness the N-methyl peaks could be used to determine the cmc by the procedure outlined above, using only relative populations. The proton NMR spectra did not show any indication of broadening. Therefore the obtained data was used for the determination of the cmc. Differences in quality compared to other measurements were not noticed. Table III contains the results of the experiment and Figure 17 was generated to determine the cmc.

TABLE III

CONCENTRATION-DEPENDENCE OF P_A OF LiOcSarc W/O SALT ADDITION

[LiOcSarc] (M)	P_A (%)
0.182	61.3
0.114	51.5
0.0700	36.3
0.0285	34.6
0.00760	35.9

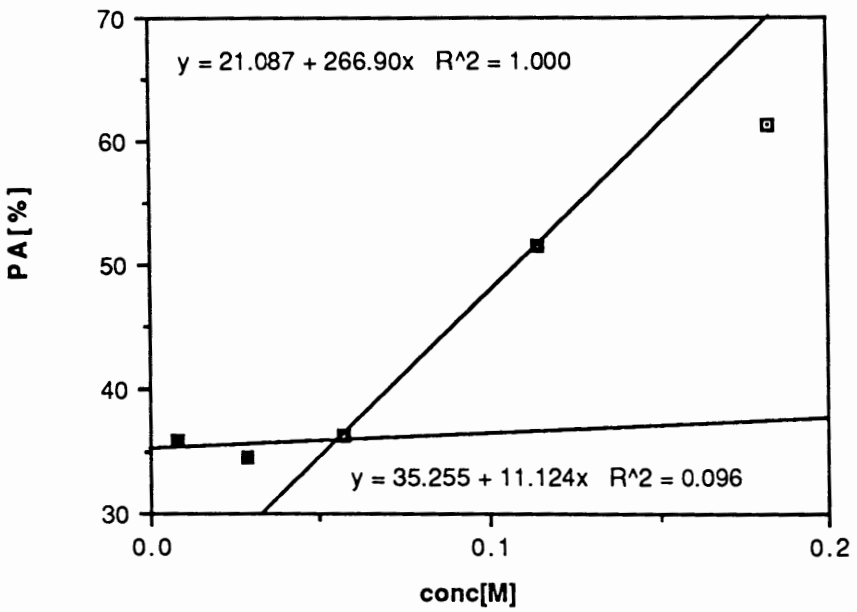

Figure 17. Cmc determination of LiOcSarc by monitoring relative populations. The resulting cmc is found to be ≈ 0.055 M.

From the graphical analysis a cmc for LiOcSarc of ≈ 55 mM. Due to the few data points around the onset of the population change the cmc is less reliable than in the NaOcSarc case. Nevertheless the clear trend to a higher cmc is visible.

Cmc of NaDecSarc w/o Salt Addition

The cmc for NaDecSarc without added salt was determined by the procedure outlined above, using only relative populations.

TABLE IV

CONCENTRATION-DEPENDENCE OF P_A OF NaDecSarc W/O SALT ADDITION

[NaDecSarc] (mM)	P_A (%)
116.0	68.6
58.0	64.5
42.9	59.4
29.0	52.2
23.2	46.9
19.3	42.0
14.5	41.1
3.9	39.7
0.95	38.5

The apparant population changes in Figure 18 even at lowest concentrations might indicate premicelle formation and make the determination of the cmc somewhat ambiguous. Although a steep rise of P_A can be seen and consequently a cmc can be determined, the precise value of the cmc remains questionable. A more thorough investigation of the observed phenomena would be necessary to elucidate if premicellization really occurs in the present case.

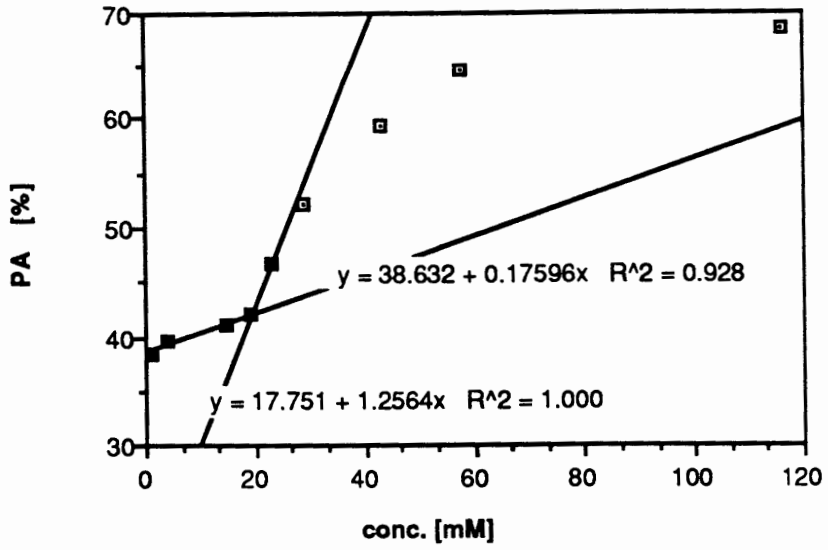

Figure 18. Cmc determination of NaDecSarc. The determined value is 19 mM.

The cmc of NaDecSarc without salt addition is 19 mM. It can be seen from Figure 18 that this particuliar case impose an interpretation where the onset of the population change is interpreted as micellization process.

Cmc of LiDecSarc w/o Salt Addition

The cmc was determined was determined by the procedure outlined above, using only relative populations. The critical micelle concentration for this molecule was determined only in the absence of added salt. Table V contains the measured data and Figure 19 indicates how the cmc was finally determined.

A summary Table of all the determined critical micelle concentration values is provided at the end of this Chapter. The summary show that the general prediction about various parameters influencing the cmc of Chapter II are useful for the studied carbamates.

An estimation of error is given at the end of Chapter IV. Although the chosen method proves to be sensitive for cmc determination, it should be pointed out that the limits of cmc value were discussed in Figure 3.

TABLE V

CONCENTRATION-DEPENDENCE OF P_A OF LiDecSarc W/O SALT ADDITION

[LiDecSarc] (mM)	P_A (%)	[LiDecSarc] (mM)	P_A (%)
64.2	68.2	22.1	51.9
53.5	66.2	20.0	51.6
45.8	65.0	10.0	39.8
37.7	63.4	5.0	38.0
32.1	60.7	2.5	39.2
27.9	58.4	0.5	40.0
24.7	56.1		

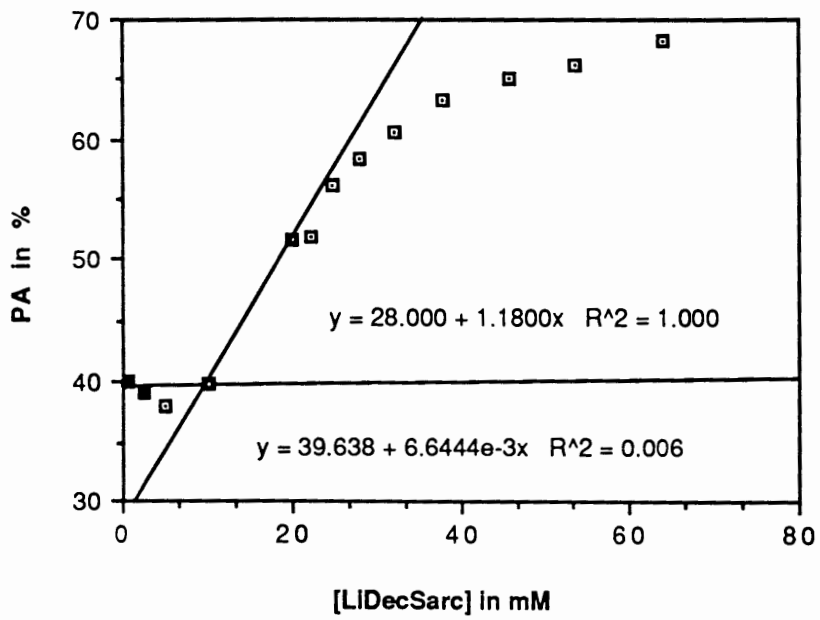

Figure 19. Cmc determination of LiDecSarc, yielding a value of 10 mM.

ASSIGNMENT OF THE N-METHYL PEAKS TO THE CORRESPONDING TRANS-, CIS- CONFORMATION

Two-Dimensional Rotating Frame Nuclear Overhauser Effect Spectroscopy (2D ROESY)

In order to determine which of the two N-methyl peaks belongs to the trans- or cis-conformation a 2D ROESY experiment (91) was performed to observe possible NOE's between the N-methyl / N-methylene and the methylene of the alkyl chain. The presence of NOE's allows an unambiguous assignment of the signal/conformation relation. NOE's depend mostly on the distance between two nuclei. The signal decreases with a distance dependence of r^{-6}. Therefore NOE's can only be observed from nuclei which are close in space (up to 5 Å) for a sufficient time. The study could not be performed on the carbamates because they do not show NOE's between the N-methyl group and the alkyl chain for two reasons.

First of all, the O-methylene group is too far in space to show a NOE to the N-methyl group, and second the rotation about the C-N bond is too fast to allow a selective NOE to build up. Therefore the corresponding amide was synthesized because it shows the same concentration dependence of the N-methyl peaks than the carbamates. The result of the 2D-ROESY experiment of SNOS is assumed to reflect the situation for the carbamates.

In Figure 22 the expected NOE's of the N-methyl group are outlined for the cis and trans conformation.Two NOE's are expected for the trans conformation and one for the cis conformation. The N-methyl peak (≈ 3 ppm) which showed only a NOE to the N-methylene group (≈ 2.5 ppm) must correspond to the cis conformation, whereas the N-methyl peak with the additional NOE to the carbonyl methylene (≈ 2.5 ppm) must correspond to the trans conformation.The expected NOE's can be tracked down in the 2D ROESY spectra for the nonmicellar (a) and the micellar (b) case indicated by the dashed lines. The result is that the downfield N-methyl peak represents the trans conformation.

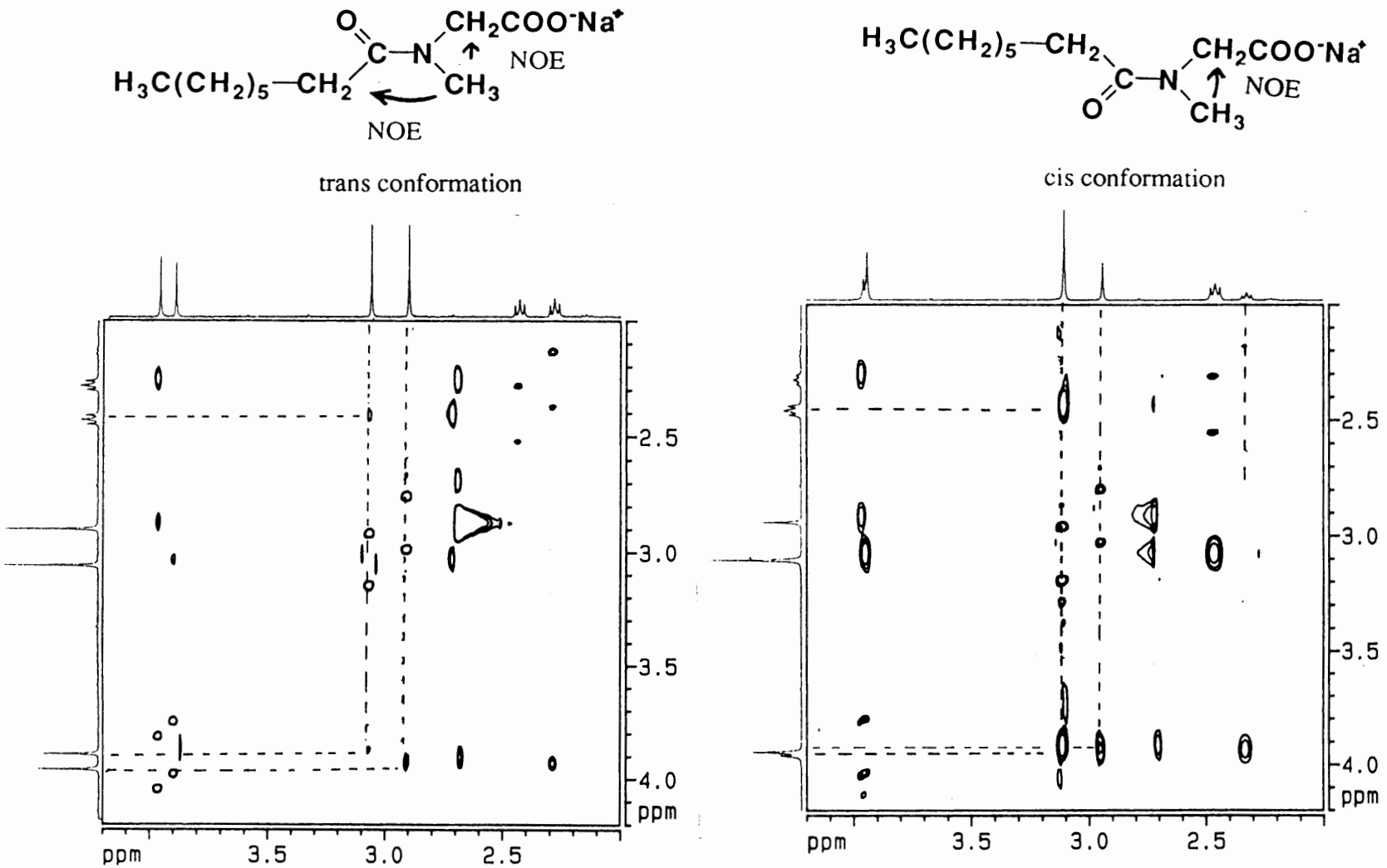

Figure 20. 2D ROESY spectra of SNOS, a. [SNOS] = 2 mM, b. [SNOS] = 2 M.

COMPUTER SIMULATION OF $\Delta H^{\ddagger}$

Computer simulation of the activation parameter of the C-N bond in NaMetSarc with the Macintosh program 'CAChe'

As an additional tool of comparison, a computer model calculation was performed. The limited reliability of this computation approach is obvious in that the calculations of the program are based on the following assumptions: 1. No solvent is included, and 2. only a single molecule in the gas phase is considered.

The molecular mechanics force field calculation was carried out for NaMetSarc. The molecule structure file contains 19 atoms, 18 bonds, and 50 connectors. Energy terms for the following interactions were included: bond stretching, bond angles, dihedral angles, improper torsions, van der Waals forces, electrostatic forces, and hydrogen bonding. The block-diagonal Newton-Raphson method was used to locate the energy minimum. Atoms were allowed to move only one at a time during energy minimization. Optimization was continued until convergence was obtained, as defined by the energy change being less than 0.001 kcal/mole in a cycle, or until the molecule was updated 300 times.

Some atoms are not parameterized in MM2, so an augmented force field was required to handle these atoms. Table VI,the following graph, and molecular structure (Figure 22 + 23) result from these calculations. The activation parameter $\Delta H^{\ddagger}$ indicates that the trans conformation is predominant, although the enthalphy difference is really very small (1.2 kcal/mol).

Surprisingly the program calculated two different energy maxima. This should ideally not be the case, because the direction of the rotation should not affect the maximum. This then shows the limits of the computer application, or that the chosen step size was too large. For the final result the average of the two bond rotational values is $\Delta H^{\ddagger}$= (24.2 + 23.6)/2 = 23.9 kcal/mol.

TABLE VI

COMPUTER SIMULATION OF THE ACTIVATION PARAMETER $\Delta H^{\ddagger}$ OF ROTATION AROUND THE CARBONYL-NITROGEN BOND IN NaMetSarc

Rotation angle (degrees)	$\Delta H^{\ddagger}$ (kcal/mol)	Rotation angle (degrees)	$\Delta H^{\ddagger}$ (kcal/mol)
0	6.0	190	7.5
10	6.2	200	8.4
20	7.2	210	9.8
30	8.7	220	11.6
40	10.6	230	13.7
50	12.7	240	15.9
60	15.2	250	18.0
70	17.7	260	20.1
80	20.2	270	21.8
90	22.4	280	23.0
100	24.0	290	23.6
110	24.2	300	20.5
120	16.2	310	13.9
130	13.2	320	10.9
140	11.1	330	8.8
150	9.5	340	7.2
160	8.2	350	6.3
170	7.4	360	6.0
180	7.2		

Plotting the calculated activation enthalphies vs the rotation angle reveals the final value.

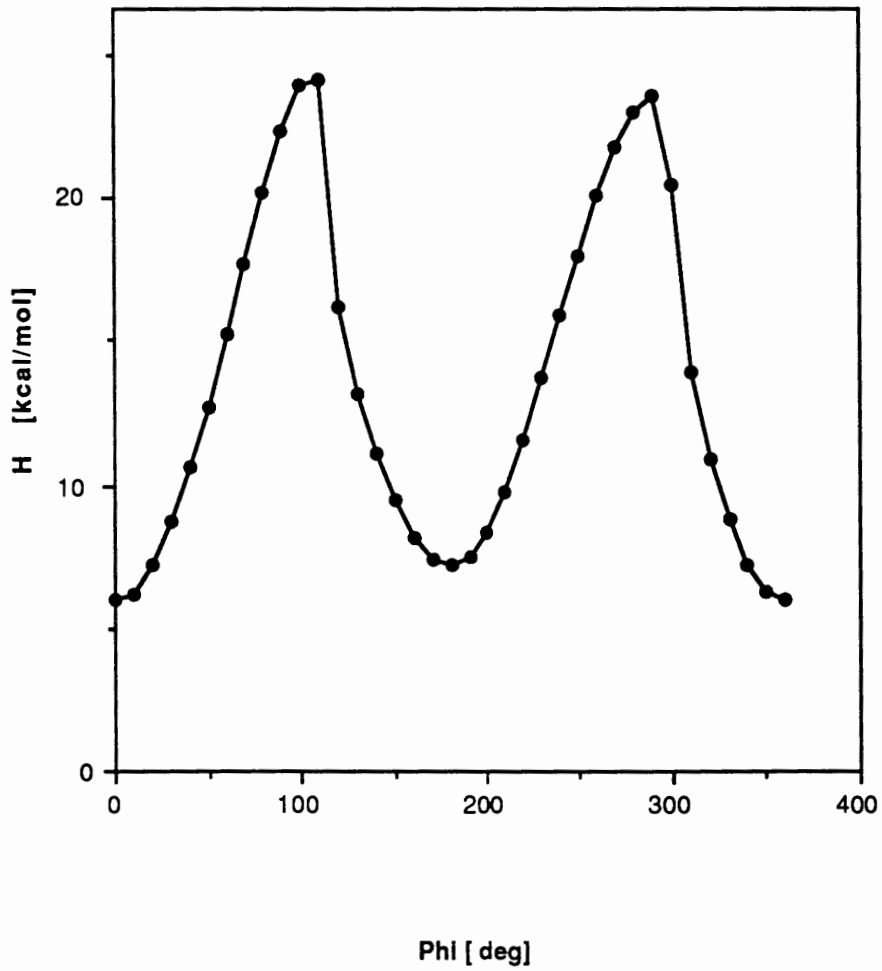

Figure 21. Graphical determination of the activation parameter $\Delta H^{\ddagger}$.

From Figure 21 the actual activation barrier of rotation was obtained by locating the energy minimum of the cis conformation. Then the two maxima were determined. It can be seen from this that first of all the two maxima are not of the same height. This setback was already predictable from Table VI. Furthermore the energy curves are not symmetrical as they should ideally be.

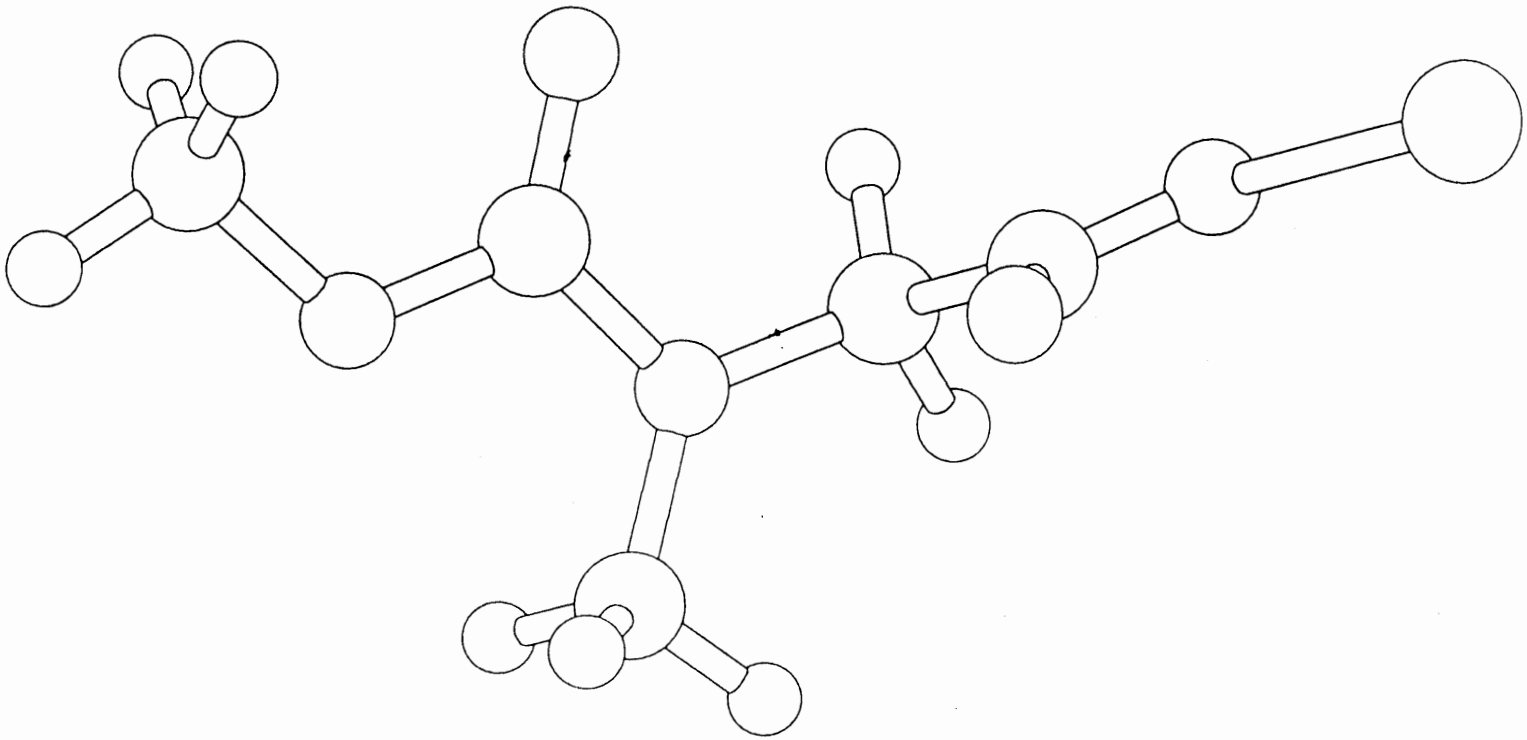

Figure 22. Calculated optimized conformation of NaMetSarc (trans).

INVERSION-RECOVERY EXPERIMENT OF NaOcSarc

In order to get an accurate value for the exchange rate (k) of the cis/trans conformers of NaOcSarc, an inversion-recovery experiment at 298 K in 2.9 ppm region of NaOcSarc (conc. = 172 mM) was made. The downfield signal was inverted with a 180°- selective pulse, then allowed to relax during different, random ordered delay times and, the recoveries of both signals were observed with time. Later lineshape analysis (92) led to τ. The results of this experiment are listed in Table VII.

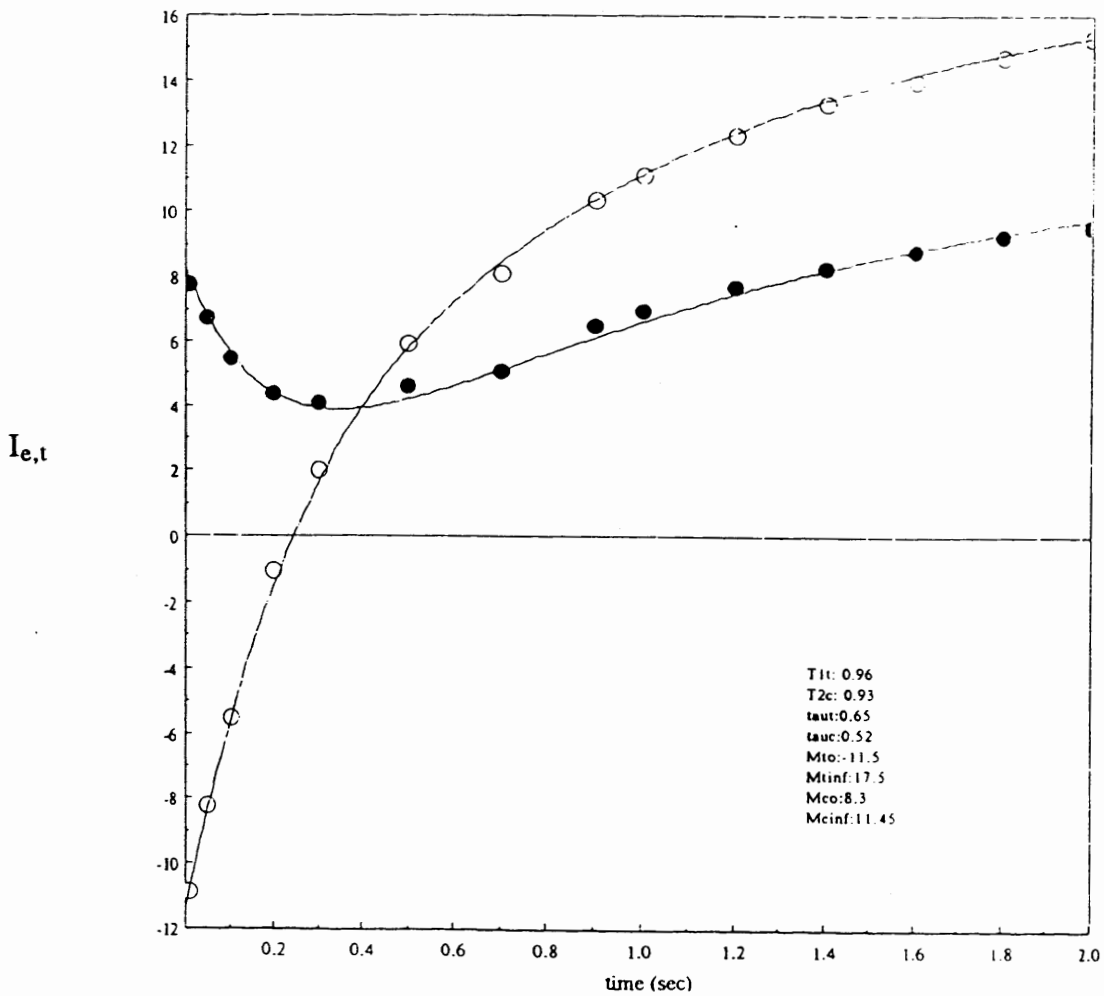

Figure 23. Results from the linefit of the inversion-recovery experiment.

TABLE VII

INVERSION-RECOVERY EXPERIMENT OF NaOcSarc

Order in which the spectra were acquired	Delay time (msec)	Peak heights (cm); Downfield/Upfield
# 1	10	-10.85/7.8
# 7	50	-8.2 /6.75
# 4	100	-5.5 /5.5
# 3	200	-1.0 /4.4
# 11	300	2.0 /4.1
# 8	500	5.95 /4.6
# 2	700	8.6 /5.6
# 9	900	10.35 /6.5
# 5	1000	11.1 /7.0
# 15	1200	12.3 /7.7
# 12	1400	13.3 /8.3
# 14	1600	14.0 /8.8
# 3	1800	14.75/9.25
# 6	2000	15.3 /9.55
# 10	10,000	18.2 /11.45

The on top shown line of fit through the data points (M;Intensity vs pulse time) led to $\tau = 0.65$ s.

DETERMINATION OF THE ACTIVATION PARAMETERS ($\Delta H^{\ddagger}$, $\Delta S^{\ddagger}$, AND $\Delta G^{\ddagger}$) OF ROTATION BY THE CBS METHOD

For all the various temperatures, a CBS analysis of the N-methyl peak was made to determine each individual τ in order to obtain the parameters of activation of rotation. The line fits lead to the indicated results. In most cases the standard deviation of the straight line which was fit through all the data points was too high to give reliable activation parameters. Therefore a second straight line was fit to a narrower temperature range, for which statements of the activation parameters can be made with the accuracy of the values decisively improved.

Not unexpectedly, the temperature range around τ_{coal} turns out to be the most reliable region in which to work. The line fits themselves are most sensitive for changes of τ in this region. Errors are discussed in the end of this Chapter.

NaOcSarc in the Micellar State

The concentration of NaOcSarc was 0.1722 M;and the pH was adjusted to 6.9. The data are plotted in Figure 24. From this plot, two sets of parameters can be obtained: $\Delta H^{\ddagger}$ = 17.2 or 21.2 kcal/mol, and $\Delta S^{\ddagger}$ = 2.6 eu or 15.0 eu. The better fit to the data corresponds to the first in each case, in which the highest and lowest temperature data points are disregarded.

The computation is illustrated by the compilation in Table VIII, which gives the parameters $T_{2A,B}$, τ (1/k), P_A, and $\Delta G^{\ddagger}$ for each data point. This last parameter must be a function of temperature, unlike $\Delta S^{\ddagger}$ or $\Delta H^{\ddagger}$.

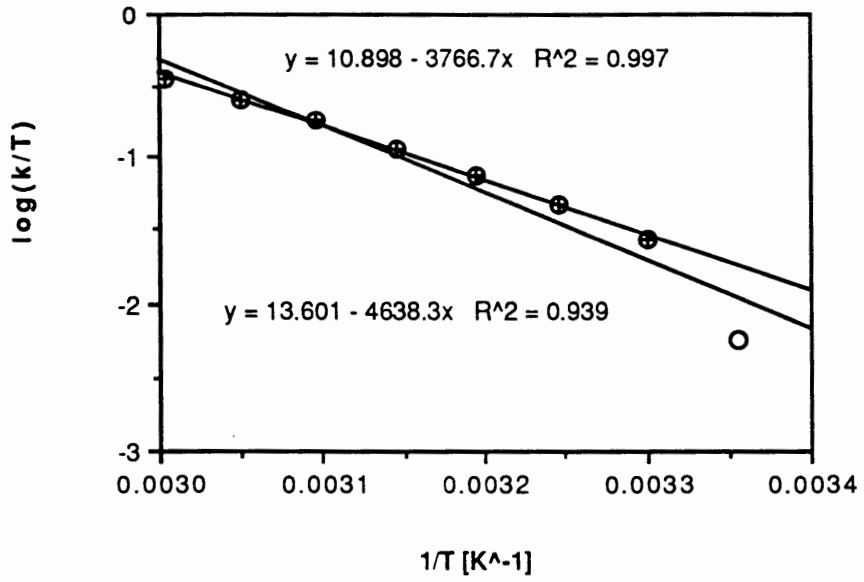

Figure 24. Determination of the activation parameters of NaOcSarc.

TABLE VIII

OBTAINED DATA FROM CBS ANALYSIS OF NaOcSarc (MICELLAR)

T (K)	T_{2A}/ T_{2B} (sec)	τ (sec)	P_A (%)	$\Delta G^{\ddagger}$ (kcal/mol)
298	0.115/ 0.115	0.6	60.5	17.1
303	0.150/ 0.155	0.12	60.0	16.5
308	0.193/ 0.193	0.069	59.9	16.4
313	0.230/ 0.230	0.0420	59.8	16.4
318	0.270/ 0.270	0.0269	59.5	16.4
323	0.310/ 0.310	0.0170	59.2	16.3
328	0.35/ 0.37	0.012	59.2	16.4
333	0.41/ 0.41	0.0082	58.7	16.4

NaOcSarc in the Micellar State (3.8ppm, N-Methylene, Region)

This was the only system where a lineshape analysis was performed on the N-methylene peaks. The reason that this experiment was performed was to allow a comparison to results from the N-methyl peaks, allowing an independent observation to see how reliable the CBS method is for this particular application.

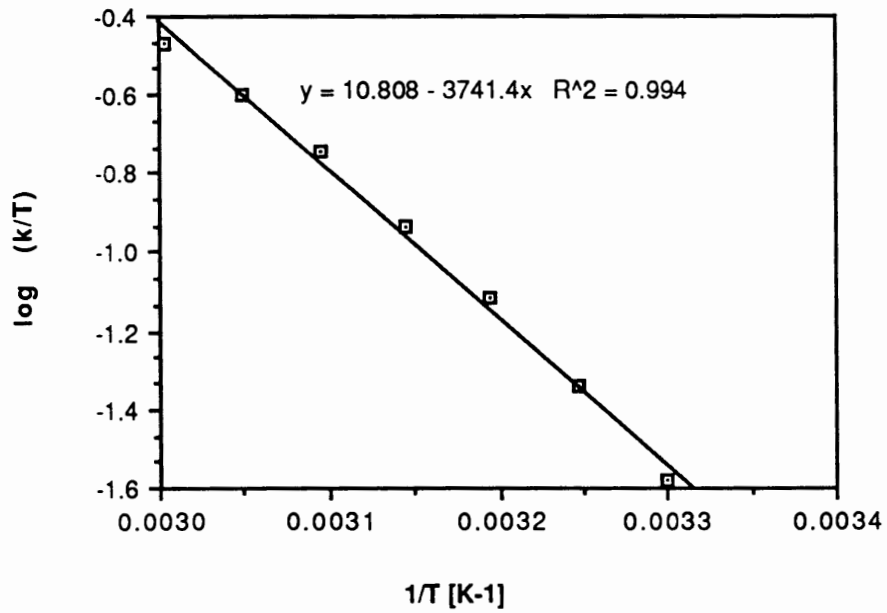

Figure 25. Determination of the activation parameters of NaOcSarc (micellar).

From the data shown in Figure 25, and from the calculations which are summarized in Table IX, values for $\Delta H^{\ddagger}$ = 17.1 kcal/mol and $\Delta S^{\ddagger}$ = 2.2 eu were obtained. In this case, there is no need to neglect any of the high or low temperature data points because the line fit is good throughout.

From these results, I conclude that the results from CBS method from either of the singlet resonances (N-methyl and N-methylene) of sarcosine can be used to gain the same result. From here on I only use the better-resolved N-methyl set.

TABLE IX

OBTAINED DATA FROM CBS ANALYSIS OF NaOcSarc (MICELLAR)

T (K)	$T_{2A/2B}$ (s)	τ (s)	P_A (%)	$\Delta G^{\ddagger}$ (kcal/mol)
303	0.120/ 0.117	0.125	41.8	16.5
308	0.145/ 0.145	0.0710	41.7	16.4
313	0.178/ 0.183	0.0415	41.4	16.4
318	0.210/ 0.216	0.0272	41.3	16.4
323	0.249/ 0.249	0.0172	41.0	16.3
328	0.295/ 0.295	0.0122	40.8	16.4
333	0.325/ 0.325	0.0088	40.6	16.4

NaOcSarc in the Nonmicellar State

The concentration of NaOcSarc was 1.7mM, and the pH was adjusted to 6.9. The resulting values were $\Delta H^{\ddagger}$(sel.) = 16.9 kcal/mol and $\Delta S^{\ddagger}$= 1.3 eu for the better line fit.

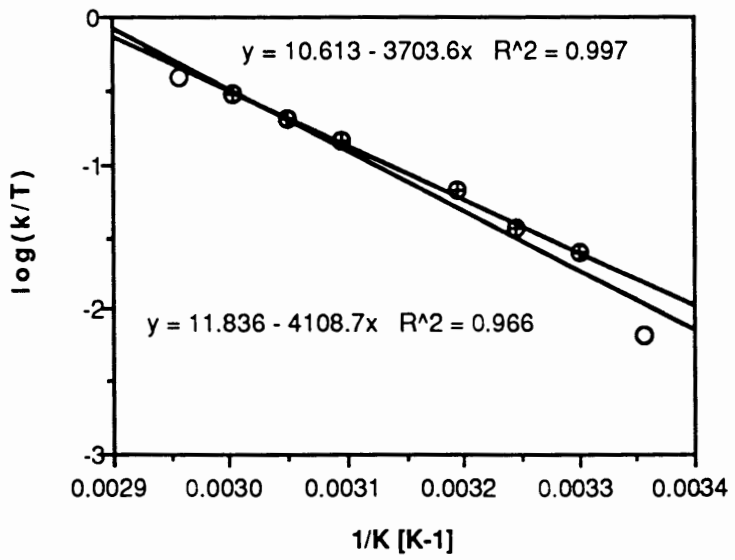

Figure 26. Determination of the activation parameter of NaOcSarc (nonmicellar).

This value is essentially the same as was seen for the micellar cases, either with or without added NaCl. This is not what Gerig et al. (8) found for the longer dodecyloxysarcosinates. The present results may reflect a less ordered micelle than was seen for the longer chain micelles.

TABLE X

OBTAINED DATA FROM CBS ANALYSIS OF NaOcSarc (NONMICELLAR)

T (K)	$T_{2A/2B}$ (s)	P_A (%)	τ (s)	$\Delta G^{\ddagger}$ (kcal/mol)
298	0.170/ 0.170	38.8	0.5	17.7
303	0.190/ 0.190	39.4	0.135	17.2
308	0.210/ 0.210	39.6	0.0900	17.2
313	0.230/ 0.230	40.2	0.0485	17.1
318	*			
323	0.270/ 0.270	40.7	0.0215	17.1
328	0.290/ 0.290	40.9	0.0146	17.2
333	0.310/ 0.310	41.3	0.010	17.2
338	0.330/ 0.330	41.6	0.0077	17.3

NaOcSarc in the Micellar State with Added NaCl (*)

The concentration of NaOcSarc was 155 mM, 30 mM of NaCl were added, and the pH was adjusted to 6.9. The data were fit to two lines, one taking into account all of the data points, and one neglecting the highest and the lowest temperatures. From this latter line fit, the activational values $\Delta H^{\ddagger}$= 17.2 kcal/mol and $\Delta S^{\ddagger}$= 2.7 eu were obtained. These values are essentially the same as without added salt (above).

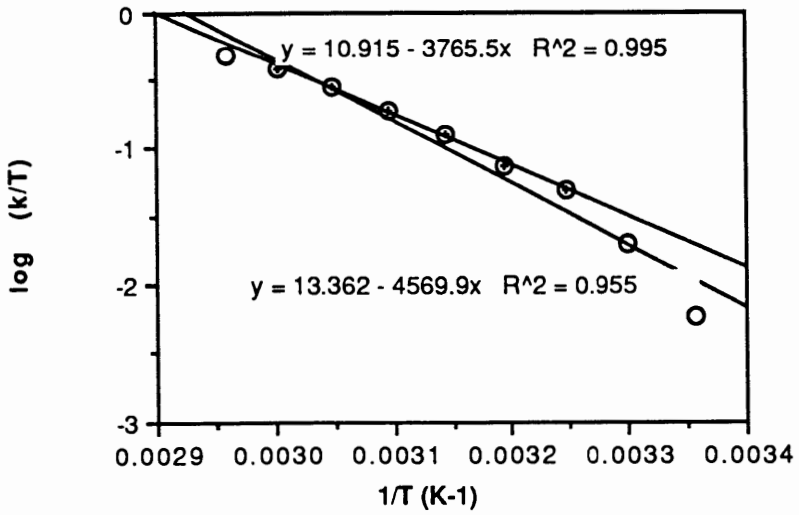

Figure 27. Determination of the activation parameters of NaOcSarc + NaCl.

TABLE XI

OBTAINED DATA FROM THE CBS ANALYSIS OF NaOcSarc (MICELLAR + SALT)

T (K)	$T_{2A/2B}$ (s)	P_A (%)	τ (s)	$\Delta G^{\ddagger}$ (kcal/mol)
298	0.115/ 0.115	66.0	0.58	17.1
303	0.150/ 0.150	65.6	0.165	16.7
308	0.198/ 0.198	65.2	0.0675	16.4
313	0.240/ 0.240	64.8	0.044	16.4
318	0.270/ 0.270	64.6	0.025	16.3
323	0.320/ 0.320	64.2	0.0162	16.3
328	0.370/ 0.370	63.8	0.0110	16.3
333	0.420/ 0.420	63.4	0.0079	16.4
338	0.470/ 0.470	63.0	0.0060	16.4

NaOcSarc in the Nonmicellar State with Salt (*)

The concentration of NaOcSarc was 1.35 mM, 30 mM NaCl were added, and the pH was adjusted to 6.9.

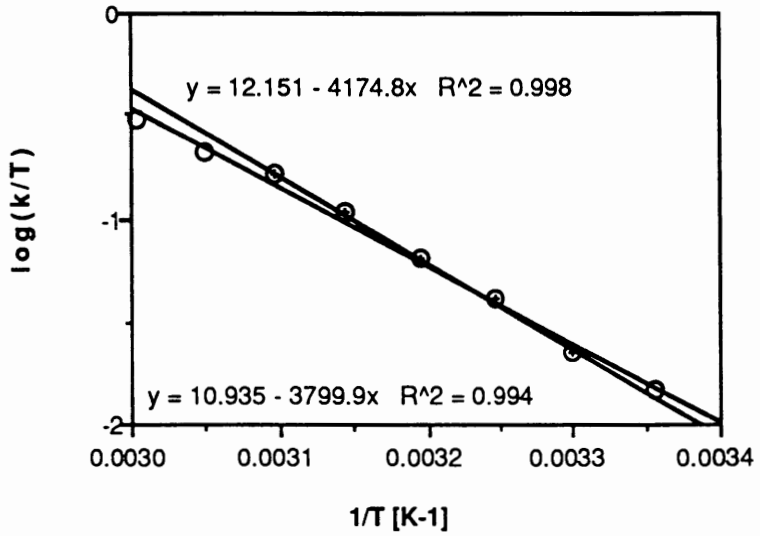

Figure 28. Determination of the activation parameters of NaOcSarc (nonmicellar +Salt).

TABLE XII

OBTAINED DATA FROM CBS ANALYSIS OF NaOcSarc (NONMICELLAR + SALT)

T (K)	$T_{2A/2B}$ (s)	P_A (%)	τ (s)	$\Delta G^{\ddagger}$ (kcal/mol)
298	0.170/ 0.170	40.5	0.23	16.6
303	0.210/ 0.200	40.5	0.145	16.6
308	0.205/ 0.205	40.6	0.0790	16.5
313	0.230/ 0.230	41.2	0.0490	16.5
318	0.240/ 0.250	41.4	0.0290	16.4
323	0.265/ 0.270	41.8	0.0190	16.4
328	0.290/ 0.290	42.2	0.0145	16.5
333	0.310/ 0.310	42.6	0.0010	16.5

The data were fit to two lines, one taking into account all of the data points, and one neglecting the two highest temperatures and the single lowest temperature. From this latter line fit, the activational values $\Delta H^{\ddagger}$= 19.1 kcal/mol and $\Delta S^{\ddagger}$= 8.4 eu were obtained. These values are not the same as without added salt (above), and seems to reflect a more ordered ground state for the system.

LiOcSarc in the Nonmicellar State

The concentration of LiOcSarc was 0.32 mM, andthe pH was adjusted to 6.9.

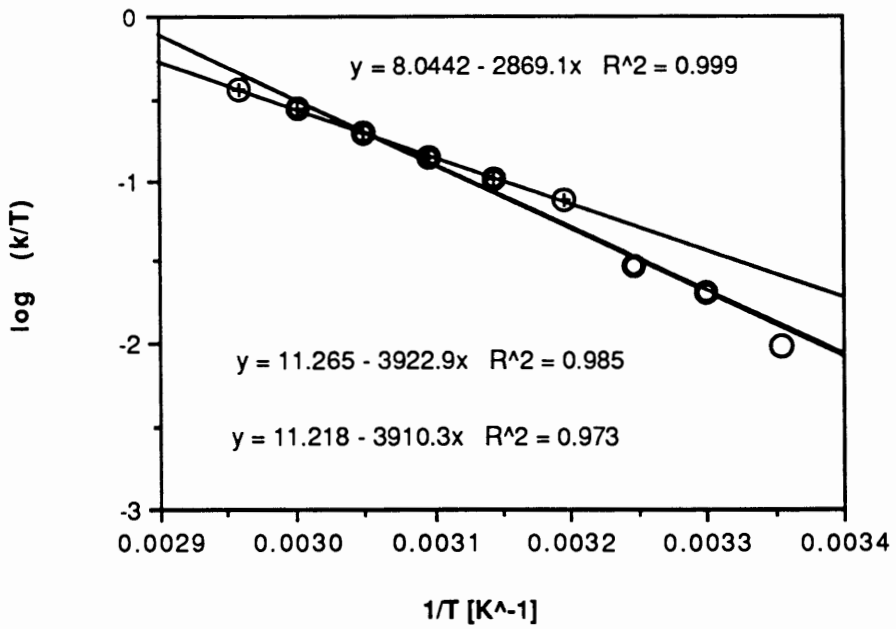

Figure 29. Determination of the activation parameter of LiOcSarc (nonmicellar).

The data were fit to three lines, two of which were nearly coincident. This case was particularly troublesome, with at least one data point near $\tau_{coalesc}$ that seems to be unreasonable. Neverthless, the two coincident lines each give what seem to be reasonable values: $\Delta H^{\ddagger}$= 17.9 kcal/mol and $\Delta S^{\ddagger}$= 4.3 eu. The alternate line, taking into account only the highest 6 data points gives $\Delta H^{\ddagger}$= 13.1 kcal/mol and $\Delta S^{\ddagger}$= -10.4 eu.

TABLE XIII

OBTAINED DATA FROM CBS ANALYSIS OF LiOcSarc (NONMICELLAR)

T (K)	$T_{2A/2B}$ (s)	P_A (%)	τ (s)	$\Delta G^{\ddagger}$ (kcal/mol)
298	0.170/ 0.180	38.5	0.35	16.8
303	0.200/ 0.205	39.0	0.16	16.6
308	0.210/ 0.220	39.5	0.110	16.7
313	0.240/ 0.250	39.7	0.0415	16.4
318	0.270/ 0.270	40.2	0.030	16.4
323	0.290/ 0.290	40.6	0.0220	16.5
328	0.310/ 0.310	41.0	0.0155	16.5
333	0.330/ 0.330	41.4	0.011	16.6
338	0.350/ 0.350	41.8	0.0082	16.6

LiOcSarc in the Micellar State (*)

The concentration of LiOcSarc was 270 mM, and the pH was 6.9.

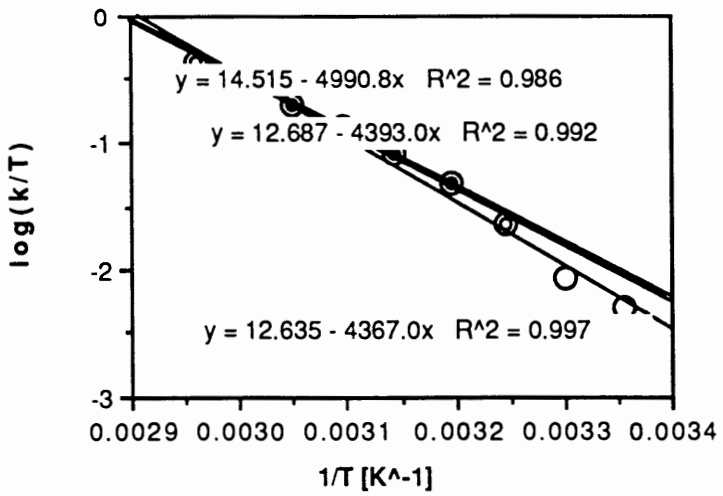

Figure 30. Determination of the activation parameter of LiOcSarc (micellar).

The data were fit to three lines. The most reasonable treatment, neglecting the highest and the three lowest temperature values, gives $\Delta H^{\ddagger}$= 20.0 kcal/mol and $\Delta S^{\ddagger}$= 10.6 eu. On the other hand, considering all of the values gives a line fit leading to activation parameters on the other extreme of $\Delta H^{\ddagger}$= 22.8 kcal/mol and $\Delta S^{\ddagger}$= 19.2 eu.

In either case, these values indicate much higher $\Delta H^{\ddagger}$ and $\Delta S^{\ddagger}$ than in the corresponding non-micellar case or for the sodium salt. Thus the presence of lithium as a counter ion increases the activational enthalpy and entropy and so seems to be an 'ordering' factor. This is not true for the nonmicellar case (above).

TABLE XIV

OBTAINED DATA FROM CBS ANALYSIS OF LiOcSarc (MICELLAR)

T (K)	$T_{2A/2B}$ (s)	P_A (%)	τ (s)	$\Delta G^{\ddagger}$ (kcal/mol)
298	0.114/0.110	65.4	0.67	17.2
303	0.125/0.138	65.2	0.38	17.2
308	0.142/0.138	66.1	0.142	16.9
313	0.155/0.155	66.3	0.0860	16.7
318	0.170/0.170	66.5	0.0385	16.6
323	0.185/0.185	66.6	0.0230	16.5
328	0.200/0.200	66.8	0.0150	16.5
333	0.215/0.215	67.0	0.0097	16.5
338	0.230/0.230	67.2	0.0067	16.5

NaDecSarc in the Nonmicellar State with NaCl

The concentration of NaDecSarc was 0.95 mM, 30 mM NaCl were added, and pH was adjusted to 6.9.

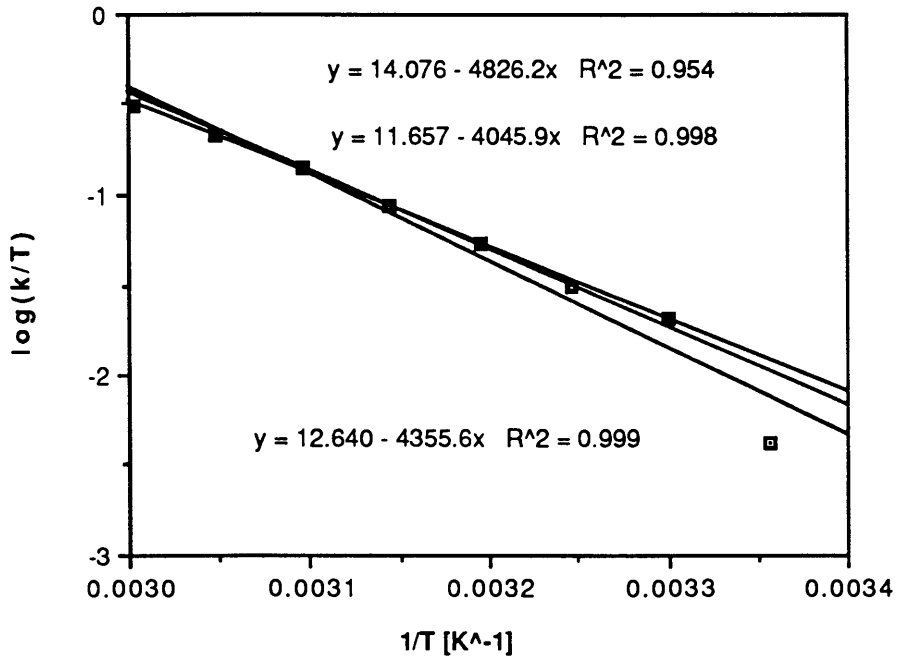

Figure 31. Determination of the activation parameters of NaDecSarc (nonmicellar).

The data were fit to three lines. The most reasonable treatment, neglecting the highest temperature value, gives $\Delta H^{\ddagger}$= 18.5 kcal/mol and $\Delta S^{\ddagger}$= 6.1 eu. On the other hand, considering all of the values gives a line fit leading to activation parameters on the other extreme of $\Delta H^{\ddagger}$= 22.1 kcal/mol and $\Delta S^{\ddagger}$= 17.1 eu.

In either case, these values indicate a slightly higher $\Delta H^{\ddagger}$ and $\Delta S^{\ddagger}$ than in the corresponding octyl case. In any event, the effect in this case seems not to be very large, especially taking the lowest slope leading to $\Delta H^{\ddagger}$ = 18.5 kcal/mol.

TABLE XV

OBTAINED DATA FROM CBS ANALYSIS OF NaDecSarc (NONMICELLAR + SALT)

T (K)	$T_{2A/2B}$ (s)	P_A (%)	τ (s)	$\Delta G^{\ddagger}$ (kcal/mol)
298	0.155/0.165	38.0	0.80	17.3
303	0.175/0.170	38.5	0.160	16.6
308	0.185/0.190	39.0	0.105	16.7
313	0.185/0.190	39.4	0.0590	16.6
318	0.210/0.210	39.9	0.0355	16.5
323	0.230/0.225	40.4	0.0220	16.6
328	0.250/0.245	40.9	0.0145	16.5
333	0.270/0.265	41.4	0.0097	16.5

NaDecSarc in the Micellar State

The concentration of NaDecSarc was 0.116 M, and the pH was adjusted to 6.9.

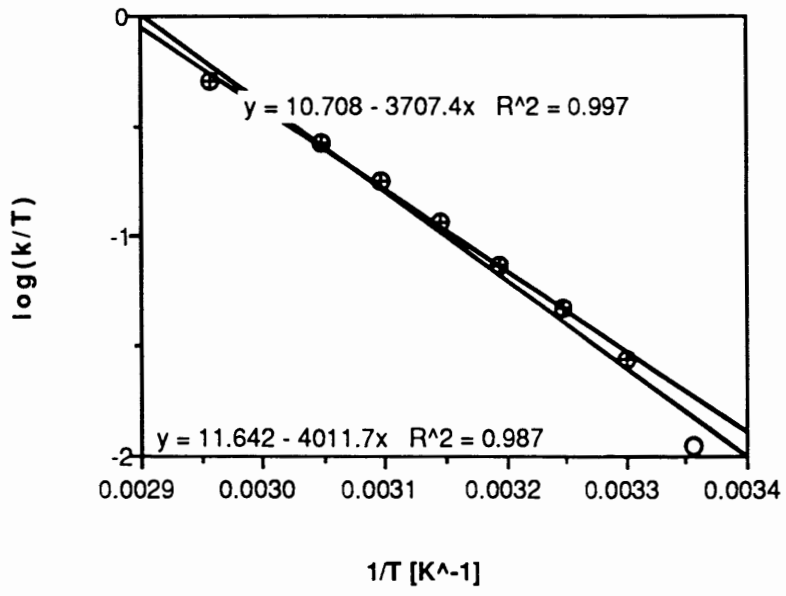

Figure 32. Determination of the activation parameters of NaDecSarc (micellar).

The data were fit to two lines. The most reasonable treatment, neglecting the highest temperature value, gives $\Delta H^{\ddagger}$= 17.0 kcal/mol and $\Delta S^{\ddagger}$= 1.8 eu. On the other hand, considering all of the values gives a line fit leading to activation parameters on the other extreme of $\Delta H^{\ddagger}$= 18.4 kcal/mol and $\Delta S^{\ddagger}$= 6.1 eu.

In either case, these values indicate a slightly higher $\Delta H^{\ddagger}$ and $\Delta S^{\ddagger}$ than in the corresponding octyl case. In any event, the effect in this case seems not to be very large, especially taking the higher slope, leading to $\Delta H^{\ddagger}$ = 18.4 kcal/mol. These values do not yet approach those of the dodecyl case as presented by Gerig et al. (8).

TABLE XVI

OBTAINED DATA FROM CBS ANALYSIS OF NaDecSarc (MICELLAR)

T (K)	T_{2A}/T_{2B} (s)	P_A (%)	τ (s)	$\Delta G^{\ddagger}$ (kcal/mol)
298	0.123/0.126	68.9	0.30	16.7
303	0.134/0.134	68.5	0.119	16.5
308	0.160/0.160	68.5	0.0690	16.4
313	0.175/0.175	68.3	0.0430	16.4
318	0.190/0.190	68.2	0.0272	16.4
323	0.210/0.210	67.9	0.0172	16.3
328	0.230/0.230	67.4	0.0114	16.3
333	0.25/0.25	66.8	0.0081	16.4
338	0.27/0.27	66.2	0.00585	16.4

HOcSarc in DMSO-d_6

The concentration of HOcSarc was 900 mM.

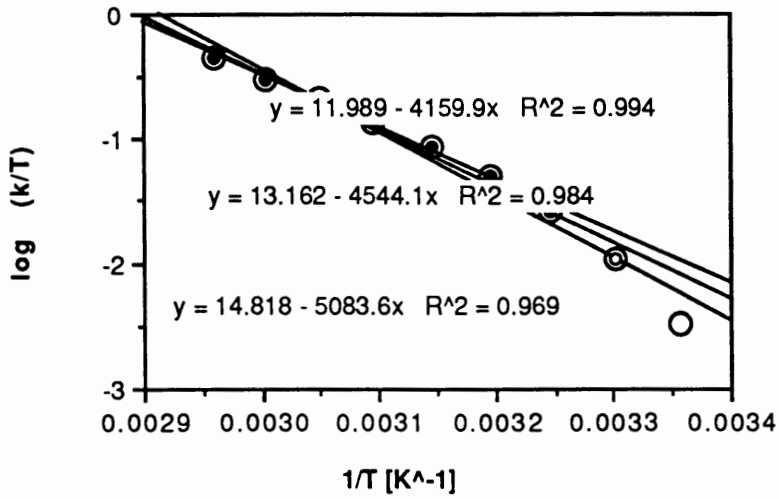

Figure 33. Determination of the activation parameters of HOcSarc.

TABLE XVII

OBTAINED DATA FROM THE CBS ANALYSIS OF HOcSarc

T (K)	T_{2A}/T_{2B} (s)	P_A (%)	τ (s)	$\Delta G^{\ddagger}$ (kcal/mol)
298	0.138/ 0.138	50.0	1.0	17.4
303	0.140/ 0.140	49.7	0.3	17.0
308	0.155/ 0.155	49.7	0.12	16.7
313	0.170/ 0.170	49.6	0.062	16.6
318	0.185/ 0.185	49.55	0.0363	16.6
323	0.200/ 0.200	49.5	0.0224	16.5
328	0.215/ 0.215	49.45	0.0145	16.5
333	0.230/ 0.230	49.35	0.0097	16.5

338	0.245/ 0.245	49.25	0.0067	16.5

The data were fit to two lines. The most reasonable treatment, neglecting the highest temperature value and lowest three temperature values, gives $\Delta H^{\ddagger}$= 18.5 kcal/mol and $\Delta S^{\ddagger}$= 6.2 eu. On the other hand, considering all of the values gives a line fit leading to activation parameters on the other extreme of $\Delta H^{\ddagger}$= 23.2 kcal/mol and $\Delta S^{\ddagger}$= 20.6 eu.

Thus, the activational parameters are similar to those of the micellar case (above). It is not so easy to interpret this result in terms of structure/order factors, however, because this molecule has a different charge than the other cases studied.

DISCUSSION OF ERROR

Estimation of the Errors in the Cmc Determinations

Accurate determination of the Cmc's proves to be a difficult project. Besides the overwhelming number of different methods that have been porposed, the delicate nature of micelle formation calls for high experimental caution and standard conditions. Basically everything effects the cmc. A good idea of the sensitivity of cmc determinations is indicated by the cmc-sensitivity toward the presence of salt. Therefore any cmc measurement is highly vulnerable to systematic as well as random errors. Preparation of the stock solution of the individual compounds is a crucial step, as is careful cleaning and rinsing of the NMR tubes.

Figure 3 suggests that the cmc is not a well defined concentration, but rather a concentration range that depends on the physical property being measured. The accuracy limit for the cmc is, according to this Figure, about 7%.

For the NMR method that I used, critical sources of error include possible impurity of the compound, and improper control of the concentration, pH, and temperature. The graphical analysis leaves also some room for interpretation. Purity of the compound was established by obtaining ^{1}H NMR spectra of the surfactants. Due to the sensitivity of the

N-methyl signal in the chosen carbamates to concentration changes, it is a good probe for micellization. On the other hand, changes of chemical shifts occur on a very small scale and so are subject to suspicion against giving reliable results. Integrals can be relied to 10% precision for the calculation of the population ratio. Clear onsets of population changes allow good graphical analysis (except NaDecSarc without added salt). The estimated error from determing the onset of the concentration dependent population changes is in my cases ± 10%.

In summary, the cmc's that I report are certainly reliable to one signficant figure. I estimate them to be within ±20%.

Estimation of Error of the Activation Parameters of Rotation

The discussion of errror has to be separated into discussions of $\Delta G^{\ddagger}$, $\Delta H^{\ddagger}$, and $\Delta S^{\ddagger}$ because they are determined differently, although they have common sources of error. Random errors sources are fluctuation in temperature and the determination of k by the CBS method itself. Systematic errors such as a general offset of the temperature are difficult to detect and exclude experimentally. The out of sequence data aquisition (indicated by *) is an attempt to decrease possible errors due to systematic heating errors or sample degredation at high temperature. The error of the temperature control unit is certainly within ± 1 K. The estimation of the error of k is more difficult.

The quality of the CBS method depends how close the system is to τ_{coal}. At τ_{coal} the fits are most reliable and show the least error. Apparantly $\Delta G^{\ddagger}$ stays almost constant throughout the whole measurements indicating that errors in $\Delta S^{\ddagger}$ and $\Delta H^{\ddagger}$ cancel themselves and leaving $\Delta G^{\ddagger}$ relatively insensitive to errors.

Applying the discussion of Sandström (11) to this study the relative error in $\Delta G^{\ddagger}$ is:

$$\frac{\Delta\Delta G^{\ddagger}}{\Delta G^{\ddagger}} = \frac{\left\{\left[\frac{\Delta T}{T}\left(\ln\frac{k_B T}{hk} + 1\right)\right]^2 + \left(\frac{\Delta k}{k}\right)^2\right\}^{1/2}}{\ln\frac{k_B T}{hk}} \qquad (13)$$

To give an estimate of the resulting error the three present extreme cases are discussed for the case of NaOcSarc (micellar, with no added salt):

Fast exchange at 338 K. ΔT is $\pm$ 1 K, Δk is $\pm$ 2.4 Hz, and k is 122 Hz. The resulting error of $\Delta\Delta G^{\ddagger}$ is then 0.3 %;

Slow exchange at 298 K. ΔT is $\pm$ 1 K, Δk is $\pm$ 0.4 Hz, and k is 2.86 Hz. The resulting error is then 0.6%;

Intermediate exchange at 318 K. ΔT is $\pm$ 1 K, Δk is $\pm$ 0.1 Hz, and k is 33.3 Hz. The resulting error is then 0.3%.

In absolut numbers the error of $\Delta G^{\ddagger}$ should not exceed 0.1 kcal/mol. To be more generous, I would assert that the reported numbers of $\Delta G^{\ddagger}$ do not exceed $\pm$ 0.2 kcal/mol.

The situation for $\Delta S^{\ddagger}$ and $\Delta H^{\ddagger}$ is somewhat different since their values were obtained by a least-squares adaptation. For reliable data the number of data points is crucial. The in most cases neglected extreme data points at the fast or the slow exchange end help to establish consistent CBS parameters in the sensitive region. The widest applicable temperature range for this experiment is 40 K. This temperature spread and sufficient data points lead to reliable data. $\Delta S^{\ddagger}$ and $\Delta H^{\ddagger}$ show high sensitivity in slight changes of k. Therefore the error on those parameters is significantly bigger than for $\Delta G^{\ddagger}$. The high correlation coefficient R (> 0.995) gives an estimated standard deviation (92) of $\pm$ 1 kcal/mol for $\Delta H^{\ddagger}$, and 2 eu for $\Delta S^{\ddagger}$. Eventual systematic errors are not included in this estimation leaving room for much caution in the Discussion section of this document. Clearly, these errors could range to as high as $\pm$ 2 kcal/mol for $\Delta H^{\ddagger}$ and $\pm$ 4 eu for $\Delta S^{\ddagger}$.

SUMMARY OF THE CALCULATED DATA

Cmc's of the Studied Systems

Table XVIII summarizes the determined cmc's. The significance is discussed in Chapter V. All the obtained and listed cmc's were produced by the same procedure. The population change of the N-methyl peak with decreasing surfactant concentration was observed. This method was favored because of its sensitivity.

TABLE XVIII

SUMMARY OF ALL THE DETERMINED CMC'S

surfactant identity	NaCl (M)	cmc (M)
NaOcSarc	0.0	0.037
NaOcSarc	1.06	0.013
LiOcSarc	0.0	0.055
NaDecSarc	0.0	0.019
LiDecSarc	0.0	0.010

Unfavorable sources of error were discussed on page 67 indicating that due to the delicate nature of the micellization process an error of ± 20% is not unrealistic. In fact such an error is for cmc studies not unusual.

This study should also show how important the control of conditions is. Slight deviations of the chosen conditions will effect the cmc. In many cases values beyond the boundary of error will result.

Activation Parameters of Studied Systems

In Table XIX the calculated activation parameters of rotation about the C-N bond are listed. The values of the most reliable fit, normally the extreme high and low temperature of the temperature NMR sets, were used for the final discussion in Chapter V.

TABLE XIX

SUMMARY OF ALL THE DETERMINED ACTIVATION PARAMETERS

surfactant identity	[surfactant] (M)	[NaCl] (M)	$\Delta G^{\ddagger}$ [2] (kcal/mol)	$\Delta H^{\ddagger}$ (kcal/mol)	$\Delta S^{\ddagger}$ (eu)
NaOcSarc	0.1722	0.0	16.4	17.2	3
NaOcSarc	0.0017	0.0	17.3	16.9	1
NaOcSarc	0.1557	0.3	16.5	17.2	3
NaOcSarc	0.0014	0.3	16.5	19.1	8
LiOcSarc	0.00032	0.0	16.4	17.9	4
LiOcSarc	0.270	0.0	16.7	20.1	10
NaDecSarc	0.116	0.0	16.4	17.0	2
NaDecSarc	0.00095	0.3	16.6	19.9	10
HOcSarc [1]	0.900	0.0	16.4	18.4	6

[1] HOcSarc was the only compound which was not studied in aqueous solution. For determining the activation parameters it was dissolved in DMSO-d_6.
[2] $\Delta G^{\ddagger}$ is reported at 40°C because the obtained k is most reliable.

An discussion of error was given on page 68. Especially $\Delta S^{\ddagger}$ is subject to cautious discussion due to its sensitive nature.

Comparison of the Population Ratios at 298 K in the Studied Systems

The significance of the population ratios listed in Table XX is given in Chapter V.

TABLE XX

SUMMARY OF THE POPULATION RATIOS OF THE STUDIED SYSTEMS AT 298 K

surfactant identity	[surfactant] (mM)	[NaCl] (mM)	P_A (%)
NaOcSarc	172	0.0	60.5
NaOcSarc	1.7	0.0	38.8
NaOcSarc	155	0.3	66.0
NaOcSarc	1.35	0.3	40.5
LiOcSarc	270	0.0	65.4
LiOcSarc	0.32	0.0	38.5
NaDecSarc	116	0.0	68.9
NaDecSarc	0.95	0.3	40.5
NaDecSarc	0.95	0.0	38.1
LiDecSarc	64.2	0.0	68.2
LiDecSarc	5.0	0.0	38.0
HOcSarc	900	studied in DMSO-d_6	50.0

Final Summary in Graphical Form

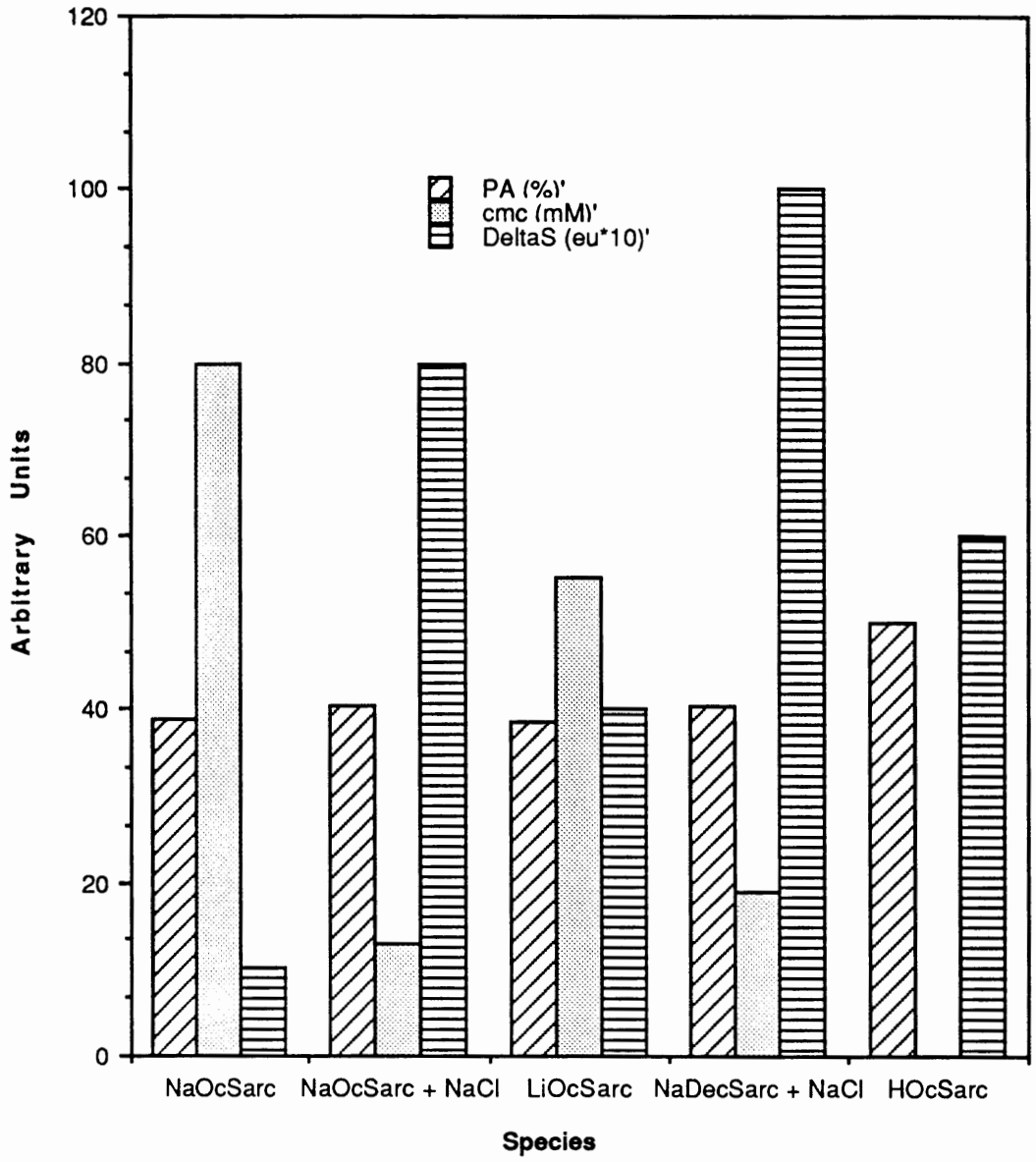

Figure 34. Summary of the obtained results for the nonmicellar species.

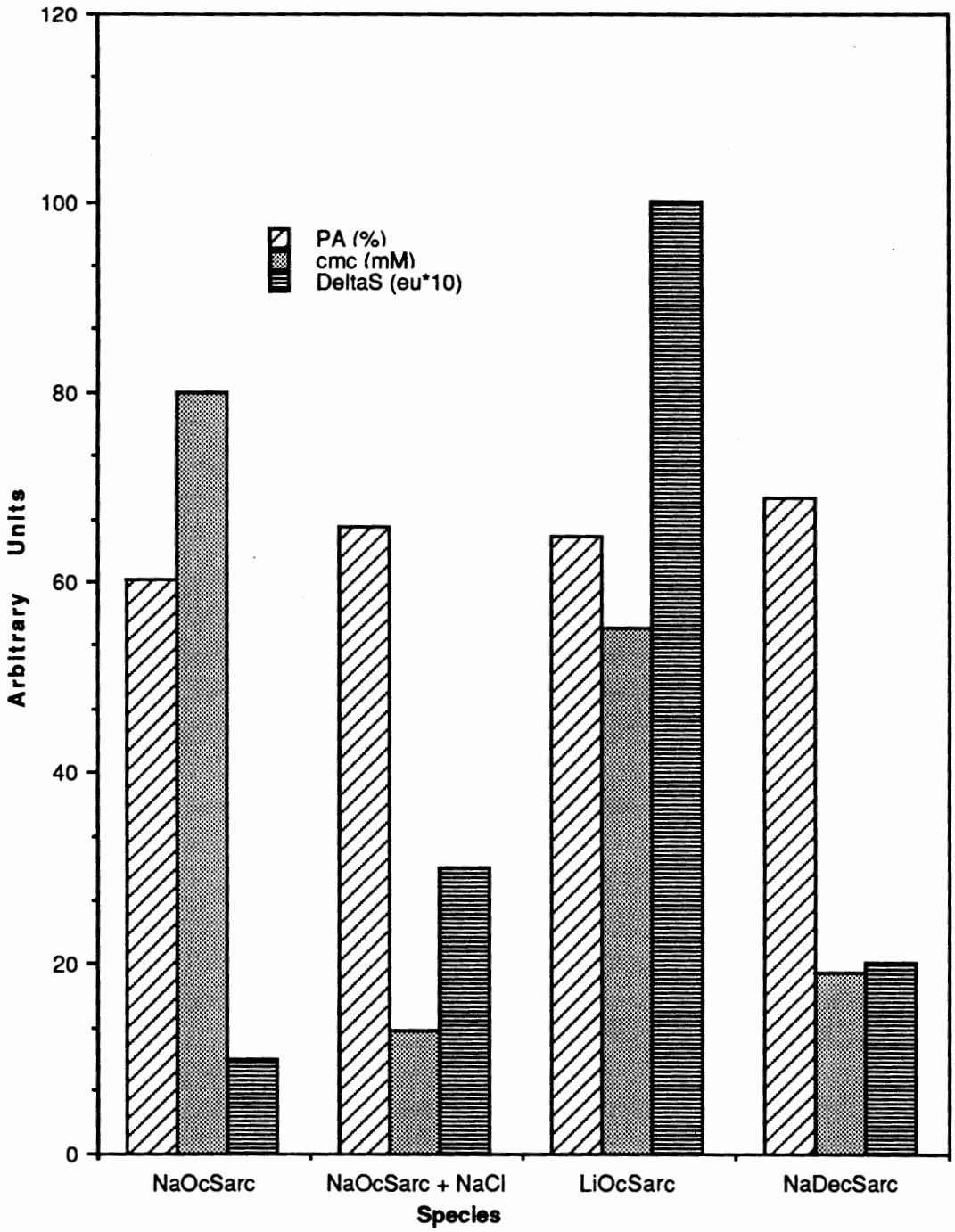

Figure 35. Summary of the obtained results for the micellar species.

CHAPTER V

DISCUSSION

HDecSarc, and HOcSarc do not show evidence for aggregation in organic solvents. Their spectra are virtually identical at different concentrations in DMSO or $CDCl_3$ as solvents. The population ratio is close to 50%, in contrast to the surfactant salts in water, suggesting that solvent-solute interactions mainly determine which conformation is favored. Formation of reversed micelles is not suspected because this would have certainly led to some sort of concentration dependence, and because this would have led to increased line widths.

The ^1H NMR spectra of NaOcSarc, LiOcSarc, NaDecSarc, and LiDecSarc each show two signals for the N-methyl group at 2.9 ppm and, less clearly, for the sarcosine methlyene group at 3.8 ppm. The signals indicate that two conformations are present. The population ratio of both sets of doublets is strongly concentration dependent, over a small concentration range. This behavior was used to determine the cmc of each compound. For SNOS the result is close to the literature value, establishing the credibility of the method. Table XVIII summarizes the obtained data. The trends of the cmc's follows basically the common rules outlined in Chapter II of the thesis. Increasing the hydrophobic chain length from eight to ten carbons decreases significantly the cmc. Exchanging the counter ion from sodium to lithium increases the cmc in the NaOcSarc case as predicted, and stays approximately the same within the given errors or slightly decreases in the NaDecSarc case. Salt addition sincerly drops the cmc which is in accordance to the rules. The obtained cmc's are therefore about what is to be expected.

The low-field N-CH_3 signal is assigned unambiguously to the trans conformer in SNOS by a 2D ROESY experiment in Figure 20, for both micellar and nonmicellar cases. This assignment is in agreement with that argued for, without coorborating data, by Takahashi et al. (7). The different population ratios in monomer and micellar states can be explained by different requirements of polarity and structure in the micellar and nonmicellar states. It appears that the more extended trans conformer, with a smaller cross section of the polar region, can be incorporated more easily in a micelle. From the molecular mechanics calculation, the trans conformation is predicted to be slighlty more stable. However this calculation does not account for solvent effects. The calculation shows that the energy difference between the two conformations is relatively small (1.2 kcal/mol). Thus, all the evidence, including the population ratios of the free acids in organic solvents (see above), indicates that the solvent environment of the surfactant plays a dominant role in determing the prefered conformation. These considerations for the amides should also apply to the corresponding carbamates, although this could not be verified in a ROESY experiment because the interconversion between the two forms is too fast, and the intramolecular distances are too large.

Computed bandshapes and subsequent calculations lead to the individual activation parameters. The selective inversion recovery experiment has good coherence with the data which were acquired by the CBS analysis, although the inversion recovery method is expected to be less accurate for this particular application.

The resulting $\Delta G^{\ddagger}$ values show are almost consistent at $\approx$ 16.5 kcal/mol, whereas $\Delta H^{\ddagger}$ and $\Delta S^{\ddagger}$ vary considerably (Table XIX). This compensation behavior is typical for entropically driven processes, suggesting that the release of structural water may play a vital role. Combining the obtained results with previous work of Gerig et al. (8), the following tendencies can be observed. All the $\Delta S^{\ddagger}$ values are positive, indicating that the rotation about the C-N is entropically favorable. Micelle formation does not seem to

influence significantly the process of rotation at a chain length of eight, or even ten carbons. This is contrary to what was found in previous work for longer chains (8). Figures 34 and 35 visualize the found results by comparing the cmc's with P_A, and $\Delta S^{\ddagger}$. Considering micellar and nonmicellar species separately, for the octyl species in aqueous solution it can be observed that with increasing relative population of site A, $\Delta S^{\ddagger}$ increases. Table XX summarizes those findings. Similar conclusions for the studied decyl species are harder to draw because they were less exhaustively studied. Nevertheless it is striking that the nonmicellar solution with high salt concentration shows a high $\Delta S^{\ddagger}$ compared to the micellar system without salt. This observation is parallel to the octyl species, suggesting same trends.

The influence of the counter ion on the activation parameters is more profound than is the actual micellization process. Tight binding of the lithium cation seems to favor the interconvertion entropically, but disfavor the process enthalpically.

The mechanism for interconversion between 1a and 1b likely does not involve a sequence in which the detergent dissociates from the micelle, rotates, and then returns to the micelle. The overall free-energy change for such a process would include the free-energy difference between micellar and nonmicellar detergent (about 2 - 4 kcal/mol in the present cases; from Equation 5 or 7) plus the barrier for rotation, known to be about 17 kcal/mol for the monomer (8) $\approx$ 20 kcal/mol. The observed values of $\Delta G^{\ddagger}$ are much smaller $\approx$ 16.5 kcal/mol, indicating a different mechanism.

Comparing 1D ^{1}H NMR spectra of micellar and nonmicellar species allows important qualitative remarks. Subtle changes in the appearance of the peak features support the physical picture of a micelle introduced in Chapter II. It is important to know that the correlation time (τ_c), corresponding approximately to the average time a molecule to progress through one radian, effects T_1 and T_2 (93); T_2 itself effects the broadness of a NMR signal. It can be said that the broadening of a peak results from a shorter T_2 due to

slower tumbling of the molecule. This qualitative tool is applied to the micellization case. The signals at ≈ 1.6 ppm and 4.0 ppm broaden significantly upon micellization, confirming the model that atoms close to the head group are hold tighter in place. The terminal methyl at 0.8 ppm is hardly effected by micellization, suggesting that it is in a fluidlike state in micelles. These findings reflect perfectly what is stated in Chapter II about the dynamics inside a micelle.

The final picture that can be given of a micelle confirm the general picture given in Chapter II, indicating a fluidity gradient increasing from the outer shell to the interior hydrophobic core of a micelle. From the study of the activation parameters extra subtlilities about the micellar structure can be suggested. Due to the position of the carbamate group close to the head, the results give information of the environment right at the borderline from the hydrophilic shell to the hydrophobic core region. The striking indifference of the activation parameters to micellization indicates that this part of the surfactant is highly exposed to the solvent result from highly disturbed spherical structures, rapid disrupture of the micelles, and fast exchange of surfactant monomers. On the other hand, some sort of micellar structure seems to remain in the short chain surfactants, as demonstrated by the broadening of the proton resonances from the alkyl chain methylenes that are α and β to the oxygen, suggesting slower tumbling resulting from formation of a micellar structure. This is also true because these molecules have a measurable cmc.

REFERENCES

1. M. J. Rosen; "Surfactants and Interfacial Phenomens", John Wiley & Sons, Inc.; (1989)

2. B. Lindman, H. Wennerström; Topics Curr. Chem.; 87, 1 (1980)

3. S. J. Ainsworth; Chem. Eng News.; 3, 27 - 63 (1992)

4. K. Shinoda; J. Phys. Chem.; 89, 2429 - 2431 (1985)

5. R. Nagarajan; Adv. Colloid Interface Sci.; 26, 205 -264 (1986)

6. R. Larter; Chem. Rev.; 90, 355 - 381 (1990)

7. H. Takahashi, Y. Nakayama, H. Hori, K. Kihara, H. Okabayashi, M. Okuyama; J. Colloid Interface Sci.; 54, 102 - 107 (1976)

8. J. T. Gerig, D. H. Peyton, D. F. Nicoli; J. Am. Chem. Soc.; 104, 5034 - 5039 (1982)

9. C. S. Johnson; Jr. Adv. Magn. Reson.; 1, 65 - 89 (1965)

10. J. Sandstöm; "Dynamic NMR Spectroscopy", Academic Press; p. 6 - 29 (1982)

11. J. Sandstöm; "Dynamic NMR Spectroscopy", Academic Press; p. 93-123 (1982)

12. B. Franklin; Philos. Trans. R. Soc. London; 64, 445 - 460 (1774)

13. Lord Rayleigh; Proc. R. Soc. London; 47, 364 - 367 (1890)

14. J. W. Mc Bain, J.T. Martin; J. Chem. Soc.; 105, 957 - 968 (1914)

15. G. S. Hartley; "Aqueous Solutions of Parafin Salts", Hermann: Paris (1936)

16. R. V. Nauman, P. Debye; J. Phys. Chem.; 53, 1 - 9 (1953)

17. P. Mukerjee, K. J. Mysels; "Critical Micelle Concentrations of Aqueous Surfactant Systems"; National Standard Reference Data Service, Vol. 36, US National Bureau of Standards, Washington, D. C.; (1971)

18. K. J. Mysels, P. Mukerjee, M. Abu-Hamdiyyah; J. Phys. Chem.; 67, 1943 - 1944 (1963)

19. B. Kraeutler, N. J. Turro; Acc Chem. Res.; 13, 369 - 377 (1980)

20. J. Deisenhofer, H. Michel; Angew. Chem. Int. Ed. Eng.; 28, 829 - 847 (1989)

21. R. Huber; Angew. Chem. Int. Ed. Eng.; 28, 848 - 869 (1989)

22. L. Kevan; in "Photoinduced Electron Transfer, part B, M. Fox, M. Chanon, Eds.; Elsevier: Amsterdam; p. 329 - 384 (1988)

23. M. N. Jones; Chem. Soc. Rev.; 21, 127 - 136 (1992)

24. J. N. Robinson, D. J. Cole-Hamilton; Chem. Soc. Rev.; 20, 49 - 94 (1991)

25. J. H. Fendler; "Membrane Mimetic Chemistry", John Wiley & Sons, Inc.; (1982)

26. H. Kuhn; Pure and Applied Chemistry; 53, 2105 - 2122 (1981)

27. A. M. Cormano-Ribeiro; Chem. Soc. Rev.; 21, 209 - 214 (1992)

28. C. Chachaty, P. Rigny; J. Chim. Phys.; 79, 203 - 226 (1982)

29. P. F. Knowles, D. Marsh; Biochem. J.; 274, 625 - 641 (1991)

30. Y. Sachor-Hill, R. G. Stullman; Biochem. J.; 31, 6272 - 6278 (1992)

31. D. R. Karsa; "Industrial Applications of Surfactants", Royal Society of Chemistry; (1987)

32. J. Falbe; "Surfactants in Consumer Products"; Springer - Verlag; (1987)

33. P. L. Layman; Chem. Eng. News.; 62, 17 - (1984)

34. R. D. Swisher; "Surfactant Biodegration", Moral Dekker, Inc.: New York, (1970).

35. J. N. Israelachvili in "Physics of Amphiphiles: Micelles, Vesicles and Microemulsions", edited by V. Degiorgio, M. Conti; Elsevier; p. 483 - 512 (1985)

36. P. Munk; "Introduction to Polymer Science", John Wiley & Sons, Inc.; (1989)

37. D. Myers; "Surfactant Science and Technology", VCH; p. 179 (1988)

38. J. H. Fendler, P. Tundo; Acc. Chem. Res.; 17, 3 - 8 (1984)

39. P. L. Luisi et al.; Biochim. Biophys. Acta; 947, 209 - 246 (1988)

40. R.J. Williams, J. N. Phillips, K. J. Mysels; Trans. Faraday Soc.; 51, 728 - 737(1955)

41. D. Myers; "Surfactant Science and Technology", VCH; p. 107 (1988)

42. B. Lindman, H. Wennerström; "Topics in current Chemistry: Micelles", VCH; 87, 11 (1980)

43. H. B. Klemens; J. Am. Oil Chem. Soc.; 30, 74 - 80 (1953)

44. M. K. Bernett, W. A. Zisman; J. Phys. Chem.; 63, 1911 - 1916 (1959)

45. B. E. Conway; "Electrochemical Data", Elsevier: Amsterdam; (1952)

46. H. J. Ache; Angew. Chem. Int. Edit.; 11, 179 - 199 (1972)

47. P. Mukerjee; Adv. Colloid Interface Sci.; 1, 241 - 253 (1967)

48. J. J. H. Nussfelder, J. B. F. N. Engbers; J. Colloid Interface Sci.; 148, 353 - 361 (1992)

49. D. F. Evans, B. W. Ninham; J. Phys. Chem.; 87, 5025 - 5032 (1983)

50. G. C. Kresheck; "Water. A Comprehensive Treatment", F. Franks Ed., Plenum: New York; Vol. 4, Chapt. 2 (1975)

51. D. Myers; "Surfactant Science and Technology", VCH; p. 82 (1988)

52. K. A. Dill, P. J. Flory; Proc. Natl. Acad. Sci. U.S.A.; 78, 676 - 680 (1981)

53. C. Tanford; "The Hydrophobic Effect: Formation of Micelles and Biological Membranes"; John Wiley & Sons, Inc., New York (1980)

54. J. N. Israelachvili in "Physics of Amphiphiles: Micelles, Vesicles and Microemulsions", edited by V. Degiorgio, M. Conti; Elsevier; p. 483 - 512 (1985)

55. D. G. Hall; Trans. Faraday Soc.; 66, 1351 - 1359 (1970)

56. D. G. Hall; Kolloid -Z.; 250, 895 (1972)

57. D. Myers; "Surfactant Science and Technology", VCH; p. 96 - 105 (1988)

58. J. N. Israelachvili; "Intermolecular and Surface Forces : with Applications to Colloidal and Biological Systems"; Academic Press (1991)

59. M. J. Vold; Langmuir; 8, 1082-1085 (1992)

60. M. J. Vold, R. D. Vold; "Colloid and Interface Chemistry"; Addison - Wesley; p. 608 (1983)

61. J. N. Israelachvili in "Physics of Amphiphiles: Micelles, Vesicles and Microemulsions", edited by V. Degiorgio, M. Conti; Elsevier; p. 46 (1985)

62. O. Glatter; Progr. Colloid Polym.; 84, 46 - 54 (1991)

63. C. Chachaty; Progr. NMR Spec.; 19, 183 - 222 (1987)

64. J. E. Baenziger et al.; Biochem. J.; 31, 3377 - 3385 (1992)

65. D. Myers; "Surfaces, Interfaces, and Colloids", VCH; p. 308 (1991)

66. M. J. Rosen; "Surfactants and Interfacial Phenomena", John Wiley & Sons: New York (1978)

68. N. J. Turro, A. Yekta; J. Am. Chem. Soc.; 100, 5951 - 5952 (1978)

69. M. J. Vold, R. D. Vold; "Colloid and Interface Chemistry"; Addison - Wesley; p. 611 (1983)

70. R. Nagarajan, K. M. Shah, S. Hammond; Colloids & Surfaces; 4, 147 - 162 (1982)

71. J. N. Israelachvili in "Physics of Amphiphiles: Micelles, Vesicles and Microemulsions", edited by V. Degiorgio, M. Conti; Elsevier; p. 42 (1985)

72. D. W. R. Gruen, E. H. B. De Lacey; "Surfactants in Solution", New York: N. Y.; 1, p. 279 (1983)

73. K. A. Dill, P. J. Flory; Proc. Natl. Acad. Sci. U.S.A.; 78, 676 -680 (1981)

74. E. C. C. Melo; J. Colloid Interface Sci; 141, 439 - 453 (1991)

75. N. Müller; J. Magn. Reson.; 28, 203 (1977)

76. B. Halle, G. Carlström; J. Phys. Chem.; 85, 2142 - 2147 (1981)

77. T. A. Holak, R. Wiltscheck, R. Ross; J. Magn. Reson.; 97, 632 - 636 (1992)

78. G. Otting et al.; J. Biomol. NMR; 1, 209 (1991)

79. H. Walderhaug, O. Södernan, P. Stilbs; J. Phys. Chem.; 88, 1655 - 1662 (1984)

80. Y. Chevalier, C. Chachaty; J. Am. Chem. Soc.; 107, 1102 -1107 (1985)

81. Y. Chevalier, C. Chachaty; J. Phys. Cem.; 89, 875 - 880 (1985)

82. K.F. Morris, C. S. Johnson, Jr.; J. Am. Chem. Soc.; 114, 3139 - 3149 (1992)

83. C. Chachaty; Prog. NMR Spectr.; 19, 183 - 222 (1987)

84. J. J. Delpuech; Analyst; 117 (3), 267 - 288 (1992)

85. A. Popov, K. Hallenga; "Modern NMR Techniques and their Application in Chemistry", Marcel Dekker, Inc. p. 521 - 566 (1991)

86. P. Baine; Magn. Reson. Chem.; 24, 304 - 307 (1986)

87. J. Sandstöm; "Dynamic NMR Spectroscopy", Academic Press; (1982)

88. W. L. Haas, E. V. Krumkalns, R. Gerzon; J. Am. Chem. Soc.; 88, 1988 - 1992 (1966)

89. F. L. Breusch; Chem. Ber.; 86, 669 - 832 (1953)

90. "Organikum", VEB Deutscher Verlag der Wissenschaften: Berlin; D. 7. 3. 4. (1986)

91. A. Bax, G. Davis; J. Magn. Reson.; 63, 207 - 213 (1985)

92. M. L. Martin, F. Mabon, M. Trierweiler; J. Phys. Chem.; 85, 76 - 78 (1981)

93. R. K. Harris; "Nuclear Magnetic Resonance Spectroscopy", John Wiley & Sons, Inc.; p. 85 - 88 (1986)

APPENDIX

The computer program used for generating the lineshapes is listed below:

```
c   Program Clatux.for classical lineshape calculation for A, B exchange.
c   Ref.: G. Binsch, Top. Steriochem. 3, 1968, ch 3, pg. 178-9.
c   Input:        free format: 'Clatux.IN'
c         # of points: NPOINT
c         Chem shift of A,B:    NEUA,NEUB
c         Linewidths:           T2A,T2B
c         population of A:      PA
c         start,end freq:       LFREQ,RFREQ
c         tau:                  TAU
c   Output:       frequency (NEU),intensity (Y)

    COMPLEX IM,AA,AB,FREQ,ALPHAA,ALPHAB,NUM,DENOM,G
    REAL STEP,PB,PA,T2A,T2B,NEUA,NEUB,LFREQ,RFREQ,TAU,NEU
    INTEGER NPOINT
    PI=3.14159
    IM=CMPLX(0.,1.)
           OPEN (UNIT=1,FILE='Clatux.IN',STATUS='OLD')
           OPEN (UNIT=2,FILE='Clatux.OUT',STATUS='NEW')
    READ(1,*)NPOINT
           READ(1,*)NEUA          !FRA
    READ(1,*)NEUB                 !FRB
    READ(1,*)T2A
    READ(1,*)T2B
    READ(1,*)PA
           READ(1,*)LFREQ         !FR1
    READ(1,*)RFREQ                 !FR2
    READ(1,*)TAU
    PB=1-PA
    STEP=(RFREQ-LFREQ)/NPOINT
    NEU=LFREQ-STEP                 !FR
    AA=-2*PI*IM*NEUA-1./T2A-PB/TAU
    AB=-2*PI*IM*NEUB-1./T2B-PA/TAU
      DO 10 I=1,NPOINT
        NEU=NEU+STEP
        FREQ=2.*PI*IM*NEU
           ALPHAA=AA+FREQ
           ALPHAB=AB+FREQ
        NUM=-IM*TAU*(2.*PA*PB-TAU*(PA*ALPHAB+PB*ALPHAA))
        DENOM=PA*PB-TAU**2*ALPHAA*ALPHAB
        G=NUM/DENOM
       Y = AIMAG(G)
    WRITE(2,*)NEU,Y
```

```
 WRITE(9,*)NEU,Y
10              CONTINUE
                STOP
                        END
```